AD-A072 862 EIC CORP NEWTON MASS F/G 10/3
INVESTIGATIONS OF THE SAFETY OF LI/SOCL SUB 2 BATTERIES.(U)
JUL 79 K M ABRAHAM, R M MANK, G L HOLLECK DAAB07-78-C-0564
UNCLASSIFIED DELET-TR-78-0564-2 NL

1 OF 1
AD A072 862

END
DATE FILMED
9-79
DDC

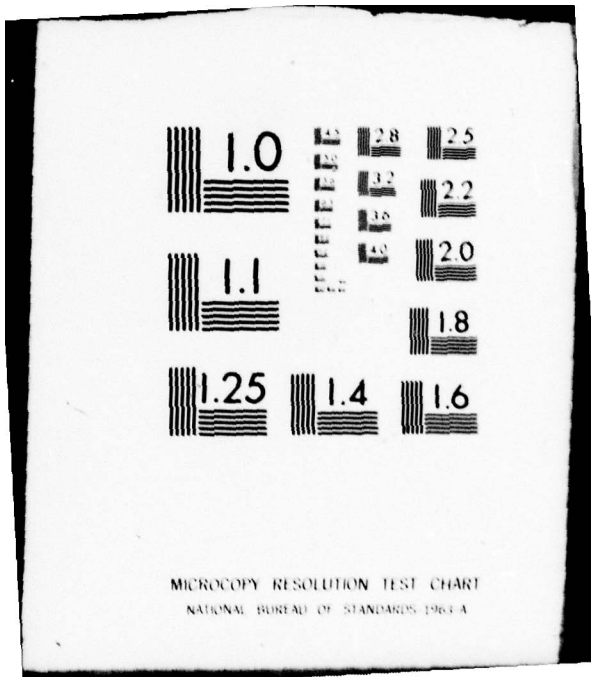
1.0
1.1
1.25
1.4
1.6
2.8
3.2
3.6
4.0
2.5
2.2
2.0
1.8
MICROCOPY RESOLUTION TEST CHART
NATIONAL BUREAU OF STANDARDS 1963 A

LEVEL II

A069797

12

Research and Development Technical Report
DELET-TR-78-0564-2

AD A072862

DDC FILE COPY

INVESTIGATIONS OF THE SAFETY OF Li/$SOCl_2$ BATTERIES

K. M. Abraham
R. M. Mank
G. L. Holleck

EIC CORPORATION
55 Chapel Street
Newton, MA 02158

July 1979

Second Quarterly Report for Period 30 Dec 78 - 30 March 79

Prepared for:
ELECTRONICS TECHNOLOGY & DEVICES LABORATORY

ERADCOM

US ARMY ELECTRONICS RESEARCH AND DEVELOPMENT COMMAND
FORT MONMOUTH, NEW JERSEY 07703

79 08 09 020

NOTICES

Disclaimers

The citation of trade names and names of manufacturers in this report is not to be construed as official Government indorsement or approval of commercial products or services referenced herein.

Disposition

Destroy this report when it is no longer needed. Do not return it to the originator.

UNCLASSIFIED

SECURITY CLASSIFICATION OF THIS PAGE (When Data Entered)

REPORT DOCUMENTATION PAGE

READ INSTRUCTIONS BEFORE COMPLETING FORM

1. REPORT NUMBER: DELET-TR-78-0564-2	2. GOVT ACCESSION NO.
3. RECIPIENT'S CATALOG NUMBER	
4. TITLE (and Subtitle): INVESTIGATIONS OF THE SAFETY OF Li/$SOCl_2$ BATTERIES.	5. TYPE OF REPORT & PERIOD COVERED: Quarterly Report No. 2, 30 Dec 1978-30 Mar 1979
	6. PERFORMING ORG. REPORT NUMBER: C-5367
7. AUTHOR(s): Kuzhikalail M. Abraham, Richard M. Mank, Gerhard L. Holleck	8. CONTRACT OR GRANT NUMBER(s): DAAB07-78-C-0564
9. PERFORMING ORGANIZATION NAME AND ADDRESS: EIC CORPORATION, 55 Chapel Street, Newton, MA 02158	10. PROGRAM ELEMENT, PROJECT, TASK AREA & WORK UNIT NUMBERS: 1L162705AH94 11-218
11. CONTROLLING OFFICE NAME AND ADDRESS: U.S. Army Electronics Research & Development Command, Attn: DELET-PR, Fort Monmouth, New Jersey 07703	12. REPORT DATE: July 1979
	13. NUMBER OF PAGES: 51
14. MONITORING AGENCY NAME & ADDRESS (if different from Controlling Office)	15. SECURITY CLASS. (of this report): UNCLASSIFIED
	15a. DECLASSIFICATION/DOWNGRADING SCHEDULE

16. DISTRIBUTION STATEMENT (of this Report)

Approved for Public Release; Distribution Unlimited.

17. DISTRIBUTION STATEMENT (of the abstract entered in Block 20, if different from Report)

18. SUPPLEMENTARY NOTES

19. KEY WORDS (Continue on reverse side if necessary and identify by block number)

Lithium thionyl chloride battery, forced overdischarge, explosion hazards, charging behavior, IR spectra, cyclic voltammetry, SO_2Cl_2, $SOCl^+AlCl_4^-$, Cl_2, Li_2S, SCl_2.

20. ABSTRACT (Continue on reverse side if necessary and identify by block number)

Cyclic voltammetry and infrared spectrometry were employed as analytical tools to characterize the reaction products in Li/$SOCl_2$ cells during various modes of operation. Sulfur dioxide is produced during the discharge. The nature of products formed during forced overdischarge depends on whether the cells are cathode or anode limited.

(continued)

DD FORM 1 JAN 73 1473 EDITION OF 1 NOV 65 IS OBSOLETE

UNCLASSIFIED 408 525

SECURITY CLASSIFICATION OF THIS PAGE (When Data Entered)

Infrared spectral data indicated that Li_2S is formed in cathode limited cells during forced overdischarge. On the other hand, there was very little or no Li_2S present in cells at the end of discharge or in anode limited cells after forced overdischarge.

From anode limited cells, Cl_2 and a compound exhibiting IR absorption at 1070 cm^{-1} were detected after forced overdischarge. These materials are formed by oxidation reactions at the anode.

Analysis of solutions from cells discharged without Li on the anode showed that SO_2Cl_2, $SOCl^+AlCl_4^-$, Cl_2, a material absorbing at 1070 cm^{-1} and probably SCl_2 are formed as oxidation products. Some SO_2 was also found in these solutions.

The products detectable after "charging" a $Li/SOCl_2$ cell were SO_2Cl_2, SCl_2, SO_2, and the material exhibiting absorption in the infrared spectrum at 1070 cm^{-1}

On the basis of materials characterized from IR spectral and cyclic voltammetry data, a mechanism is proposed for the oxidation reactions in $SOCl_2/LiAlCl_4$ solutions.

TABLE OF CONTENTS

LIST OF ILLUSTRATIONS

LIST OF ILLUSTRATIONS
(continued)

LIST OF ILLUSTRATIONS
(continued)

LIST OF TABLES

I. INTRODUCTION

In recent years there has been considerable research and development on ambient temperature, high energy density Li cells. A particularly promising system is based on $SOCl_2$ (1,2). Here, $SOCl_2$ serves as both a solvent and depolarizer for the cell. These cells have delivered 100 Whr/lb and 40 W/lb at the 2.5-hour rate and, as usual, higher energy densities at lower discharge rates (3). According to one report (4) they can deliver as much as 300 Whr/lb at low rates. Clearly this is a very promising system with many applications where high energy density and high rate are required.

The cell has two problems: (1) under a variety of circumstances, the cell has shown a tendency to explode, (2) after high temperature storage, it shows voltage delay.

The objective of this program is to explore the causes and find solutions to the explosion hazards in the Li/$SOCl_2$ cells. Three types of explosion have been reported: (1) cells explode on short circuit; (2) cells explode on forced overdischarge; (3) cells explode on resistive load overdischarge. Clearly, any high rate, high energy density system such as Li/$SOCl_2$ has the possibility of a thermal runaway type of explosion. It is not surprising that a hermetically sealed D-cell, which can deliver in excess of 20 amps, might explode when short circuited -- it just is not possible to remove the waste heat. However, this problem appears to have been solved with low pressure vents (100-300 psi) and with appropriate fuses incorporated into the cell (5,6).

The other two types of explosion are of greater concern. The forced overdischarge situation may be experienced by a cell in a battery package. Explosion on resistive load overdischarge implies that any completely discharged cell still connected to a piece of equipment is a hazard. No clear documentation of the explosion hazard on resistive load overdischarge is found in the literature. Forced overdischarge explosions have been documented for D-size (5) and C-size (10,11) Li/$SOCl_2$ cells. This type of explosion, occurring after cell-voltage reversal, takes place without prior temperature or pressure rise and appears to be chemical in its origin. We have shown that forced overdischarge explosions appear to occur only in anode limited cells (10,11). Individual electrode potential measurements during discharge and overdischarge showed that the anode was at $\geq$ 4.0V for a considerable length of time prior to an explosion. The nature of the explosion suggests the production of sensitive chemicals by oxidation of $SOCl_2$ or other materials present in the cell which could explode under certain conditions.

In order to characterize the material(s) responsible for explosion in anode limited cells, a considerable amount of analytical work was carried out during the present quarter. Major emphasis was placed on cyclic voltammetry and infrared spectroscopy.

II. CYCLIC VOLTAMMETRY STUDIES

1. Experimental Procedures

All the experiments involving reagent handling and cell construction were carried out in the absence of air and moisture in an argon atmosphere using a Vacuum-Atmospheres Corporation dry box.

Cyclic voltammetric studies of $SOCl_2/LiAlCl_4$ (1.8M) solutions were carried out on nickel and carbon electrodes using a three electrode system. A 15 mil lithium ribbon pressed onto a nickel screen served as the reference electrode. The reference electrode was contained in a Luggin capillary and was placed close to the working electrode. The counter electrode consisted of a piece of Li ($\sim$1 cm^2) pressed onto a nickel screen. The Ni working electrode consisted of a 0.5 cm^2 nickel disc (10 mil thick), fitted in a Teflon holder. The carbon working electrode was a 0.10 cm^2 glassy carbon surface. The electrodes were arranged in a 25 ml capacity, three-necked flask. A volume measuring 7 ml of $SOCl_2$/1.8M $LiAlCl_4$ solution was used. The voltammetric scans were performed with a Amel Model 551 potentiostat in conjunction with their Model 566 function generator. The i-E curves were recorded on a Houston Omnigraphic Model 2000 X-Y Recorder or on a Bascom-Turner Series 8000 Recorder provided with microprocessor capabilities.

Cyclic voltammetry of materials from discharged or overdischarged cells was carried out in situ. The experimental details are given in the next Section.

2. Cyclic Voltammetry in $SOCl_2/LiAlCl_4$ Solutions

A typical cyclic voltammogram between 1 and 5V vs. Li^+/Li in $SOCl_2$/1.8M $LiAlCl_4$ on a glassy carbon electrode is shown in Figure 1. A similar voltammogram was obtained also on a Ni electrode and is shown in Figure 2. Although the overall features of the voltammogram are identical on both of the electrodes, the peaks appeared more sharp on the carbon electrode. Also the peaks on Ni are shifted to slightly lower potentials. Therefore most of the studies were performed using the glassy carbon electrode.

2.1 Electrochemical Reduction of $SOCl_2/LiAlCl_4$ Solutions

- Experimental Results

A typical cyclic voltammogram in $SOCl_2$/1.8M $LiAlCl_4$ solution, obtained by scanning the carbon electrode cathodically from open circuit voltage (3.6V vs. Li^+/Li) is shown in Figure 3. The scan rate is 0.1V/sec. The onset of a reduction peak occurs at $\sim$3.0V with a peak at 2.6V. This reduction peak may be regarded as due to the reduction of $SOCl_2$ and is in good

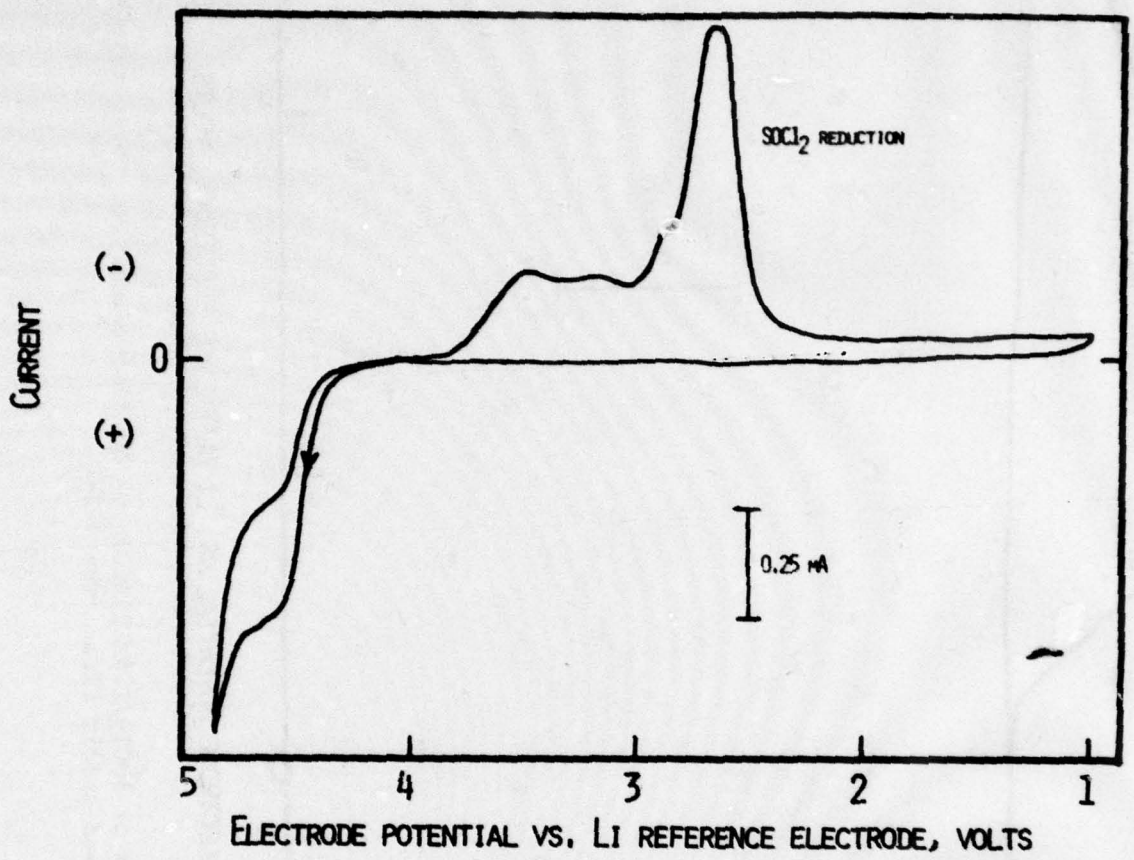

Fig. 1. Cyclic voltammograms of $SOCl_2$/1.8M $LiAlCl_4$ on glassy carbon electrode. Scan rate = 100 mV/sec. The electrode was scanned anodic first from 3.7V.

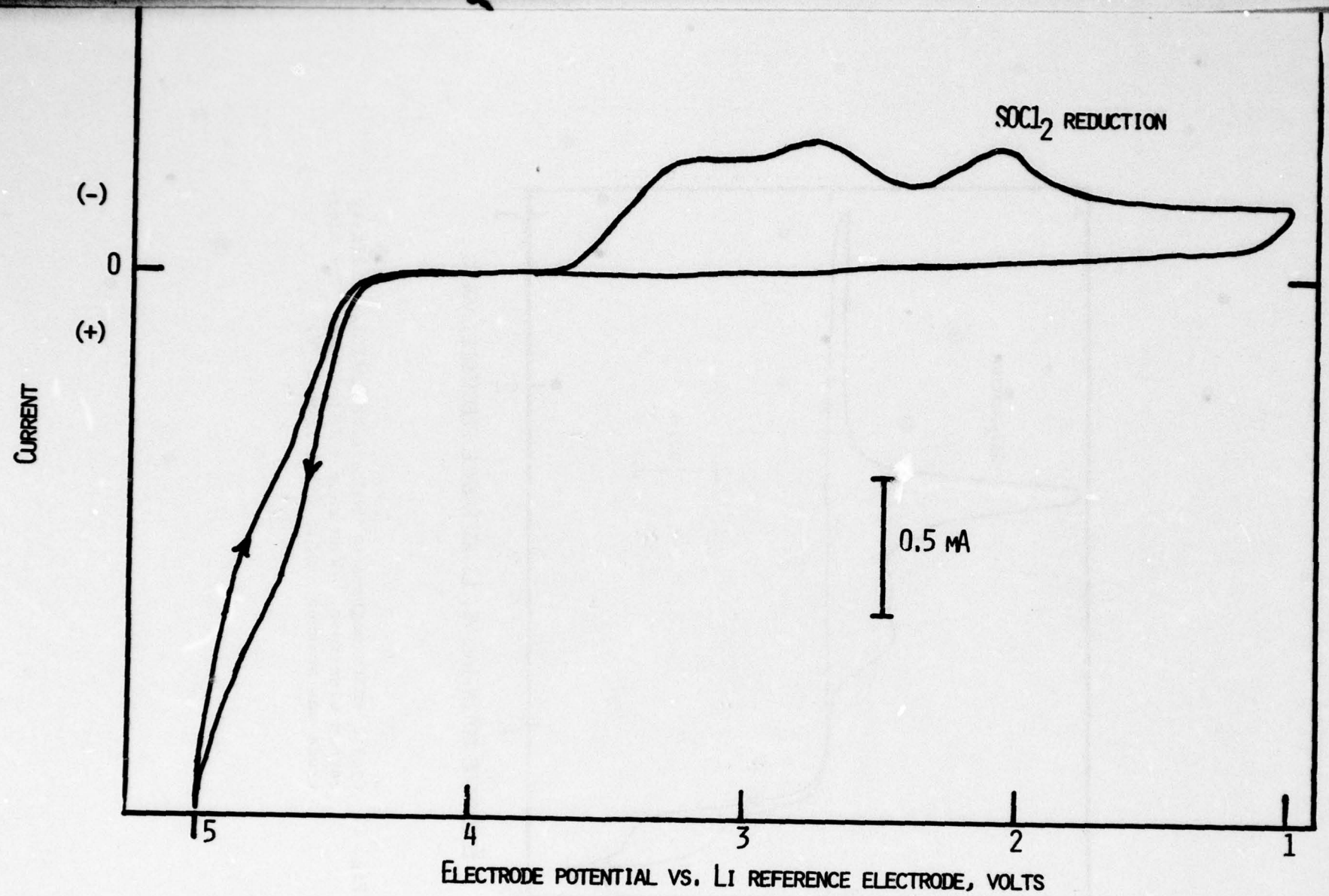

Fig. 2. Cyclic voltammogram of $SOCl_2$/1.8M $LiAlCl_4$ on Ni disc electrode. Scan rate = 50 mV/sec. Electrode was scanned anodic first from 3.7V.

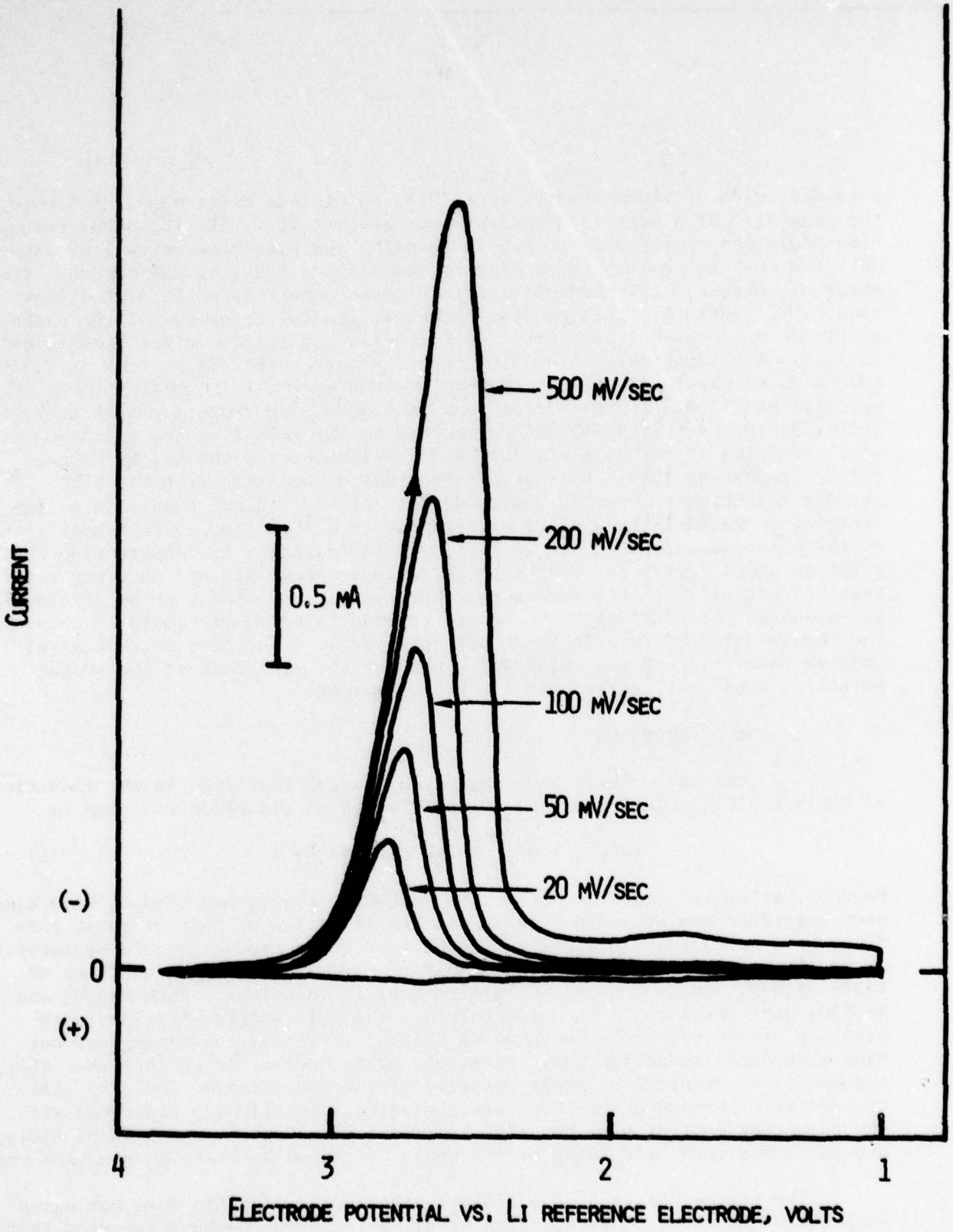

Fig. 3. Cyclic voltammogram of $SOCl_2$/1.8M $LiAlCl_4$ on glassy carbon electrode between 3.8V and 1V as a function of scan rate.

agreement with previous observations (7,8) on similar electrodes. Following the peak at 2.6V a very weak current peak appears at ∿1.8V. No other reduction peaks are observed up to 1.0V. Scanning the electrode below 1.0V showed only the current peak corresponding to the plating of Li on the carbon. The onset of current corresponding to this process occurs at ∿0.5V with a peak near 0.0V, Figure 4. This process, however, led to the damage of the carbon electrode surface and therefore in all studies the electrode was scanned only to 1.0V. The anodic scan from 1.0V showed a very weak current peak at 2.55V, and as shown previously (7), this peak may correspond to the oxidation of the material exhibiting the reduction peak at 1.80V. The reduction peak at 1.8V and oxidation peak at 2.55V may correspond to the reduction and oxidation of SO_2. Addition of SO_2 to the solution slightly enhanced the height of the reduction peak at 1.8V. Because of electrode passivation from the high current reduction process at 2.6V, addition of SO_2 did not result in a significant increase in the height of the peak at 1.8V. The severe passivation of the electrode, probably due to LiCl, was indicated by the observation that after an anodic sweep to 3.6V, second cathode sweep did not show any reduction peak at all. It was necessary to regenerate the electrode by holding it at an anodic potential of ∿4.6V before reproducible results could be obtained. The regeneration of the electrode was achieved in a second electrochemical cell so that products generated while holding the electrode at the anodic potential would not contaminate the test solution.

- Discussion

Various workers have suggested several reactions in the reduction of $SOCl_2/LiAlCl_4$ solutions. The commonly accepted reduction reaction is

$$2SOCl_2 + 4Li \rightarrow 4LiCl + SO_2 + S \qquad (1)$$

However, other reduction products such as S_2Cl_2, Li_2SO_3 and $Li_2S_2O_4$ have also been suggested and sporadic reports of identification of some of these products have appeared. In order to see whether these products could be identified by cyclic voltammetry, cyclic voltammograms were obtained with addition of S_2Cl_2 $Na_2S_2O_4$ and Na_2SO_3 to $SOCl_2$/1.8M $LiAlCl_4$ solutions. Both Na_2SO_3 and $Na_2S_2O_4$ were insolube in the electrolyte. The voltammogram obtained with addition of ∿10 v/o S_2Cl_2 is shown in Figure 5. The voltammogram does not show a separate reduction peak corresponding to S_2Cl_2. It appears that S_2Cl_2 reduces at a potential slightly positive of the reduction of $SOCl_2$ so that the positive portion of the $SOCl_2$ reduction peak is slightly broadened with the resulting current peak becoming asymmetrical. Further addition of S_2Cl_2 brought about more broadening of the $SOCl_2$ reduction peak at the positive region.

The present value of the reduction potential of S_2Cl_2 does not agree with the value reported by Blomgren et al. (8). These authors reported that S_2Cl_2 in $SOCl_2/LiAlCl_4$ solution reduces at 3.4V vs. Li^+/Li.

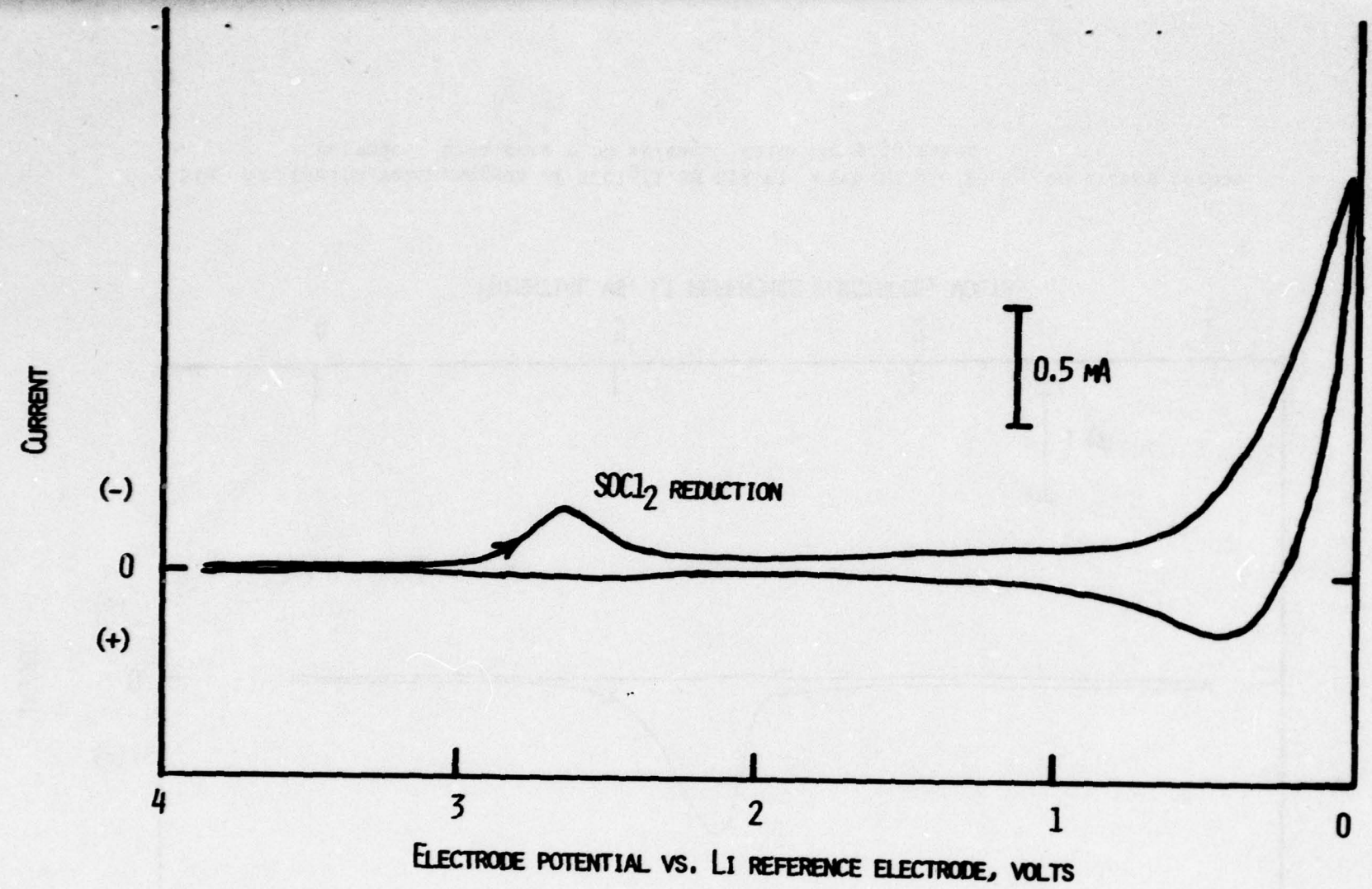

Fig. 4. Cyclic voltammogram of $SOCl_2$/1.8M $LiAlCl_4$ on glassy carbon electrode between 0.0 and 4V. Scan rate = 50 mV/sec.

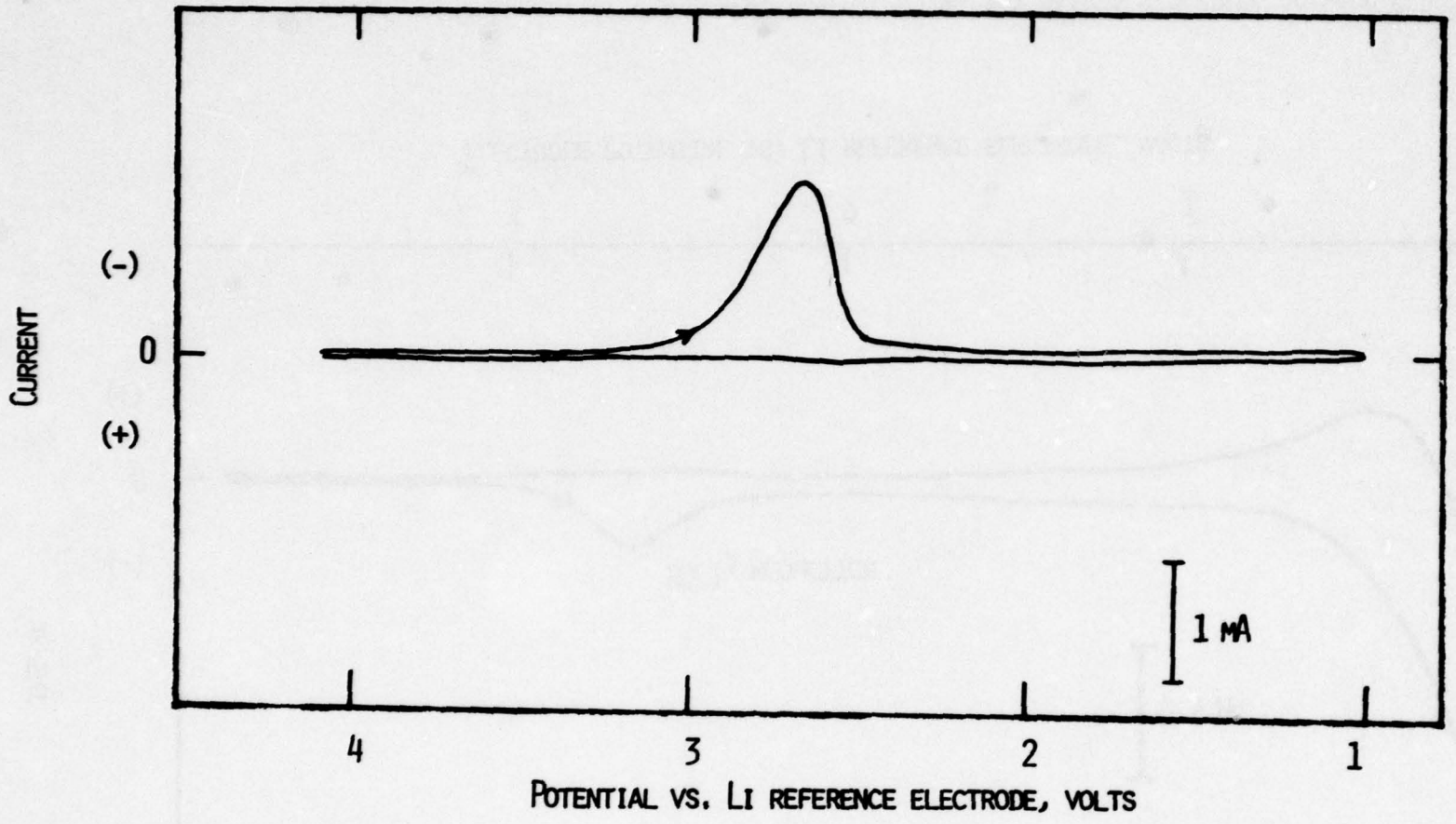

Fig. 5. Cyclic voltammogram of $SOCl_2$/1.8M $LiAlCl_4$ with 10 v/o S_2Cl_2 on glassy carbon electrode. Scan rate = 50 mV/sec. Cathodic scan first.

2.2 Electrochemical Oxidation of $SOCl_2/LiAlCl_4$ Solutions

- **Experimental Results**

A typical cyclic voltammogram in $SOCl_2$/1.8M $LiAlCl_4$ solution on a carbon electrode is shown in Figure 6. A similar voltammogram was also obtained on a nickel electrode. On scanning the electrode anodically from 4 volts, the onset of an anodic current occurs at ∿4.4V vs. Li^+/Li. The voltammogram shows two broad peaks at 4.55V and 4.65V as well as a sharp and high current peak at 5.0V. In poorly resolved voltammograms, the two peaks at 4.55V and 4.65V merge together and appear as one peak. On cycling the electrode continuously between 4 and 5 volts the heights of the broad peaks decreases although it does not completely disappear even after several cycles. After the electrode was scanned cathodically to 2V or below, a very large current peak is observed in the subsequent anodic sweep to 5.0V. In these cases, the two peaks at 4.55 and 4.65 volts generally appear as a single peak.

When the electrode is scanned cathodically below 4V after the anodic scan to 5V, the reduction peaks due to the oxidation products appear in the resulting voltammogram. It is shown in Figure 7.

There are two clearly separated current peaks at ∿3.6V and ∿3.25V which come from the reduction of oxidation products. There is also a third peak at 2.95V, appearing as a shoulder to the $SOCl_2$ reduction peak at 2.6V. These peaks are not found in the voltammogram when the first sweep was initiated cathodically from open circuit. The appearance of these peaks and their relative peak heights were found to depend on the potential of scan reversal.

None of these three peaks appear when the scan is reversed at potentials below 4.2 volts. When the scan is reversed at ∿4.6 volts the peak at 3.25 volts appears as the major one. On increasing the reversal potential to values greater than 4.6V the height of the peak at 3.6V also increases along with the appearance of the shoulder at 2.75V. If the electrode is cycled several times between 4V and 5V before sweeping cathodically, all three peaks show increased peak heights. The voltammograms obtained by addition of Cl_2 to the $SOCl_2$/$LiAlCl_4$ showed an increase in the reduction current peak at 3.25V. As would be seen later the reduction peak at 3.25V was also observed in the cathodic region of $SO_2Cl_2/LiAlCl_4$ solutions after an anodic scan to 5.0V.

In order to identify the other reduction peaks in the voltammogram resulting from oxidation products, the electrode was scanned cathodically from open circuit after adding various reagents to $SOCl_2/LiAlCl_4$ solutions. The materials added were SCl_2, S_2Cl_2, SO_2Cl_2, SO_2, $AlCl_3$ and various combinations of these. Runs were also made using the $Li_2O/AlCl_3$ based electrolyte (9) in place of $LiAlCl_4$.

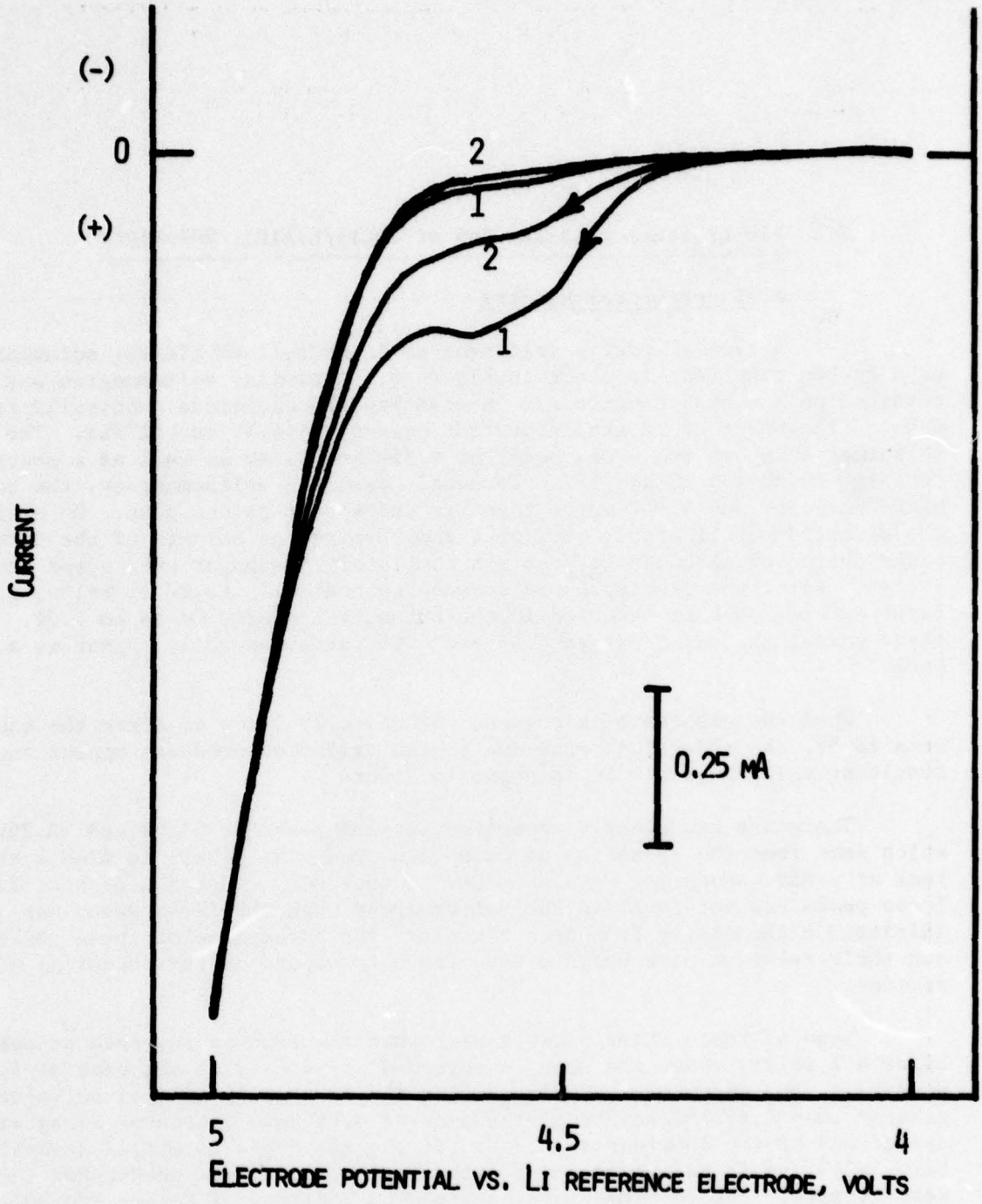

Fig. 6. Cyclic voltammogram of $SOCl_2$/1.8M $LiAlCl_4$ on glassy carbon electrode between 4 and 5 volts. Curves 1 and 2 represent successive scans. Scan rate = 50 mV/sec.

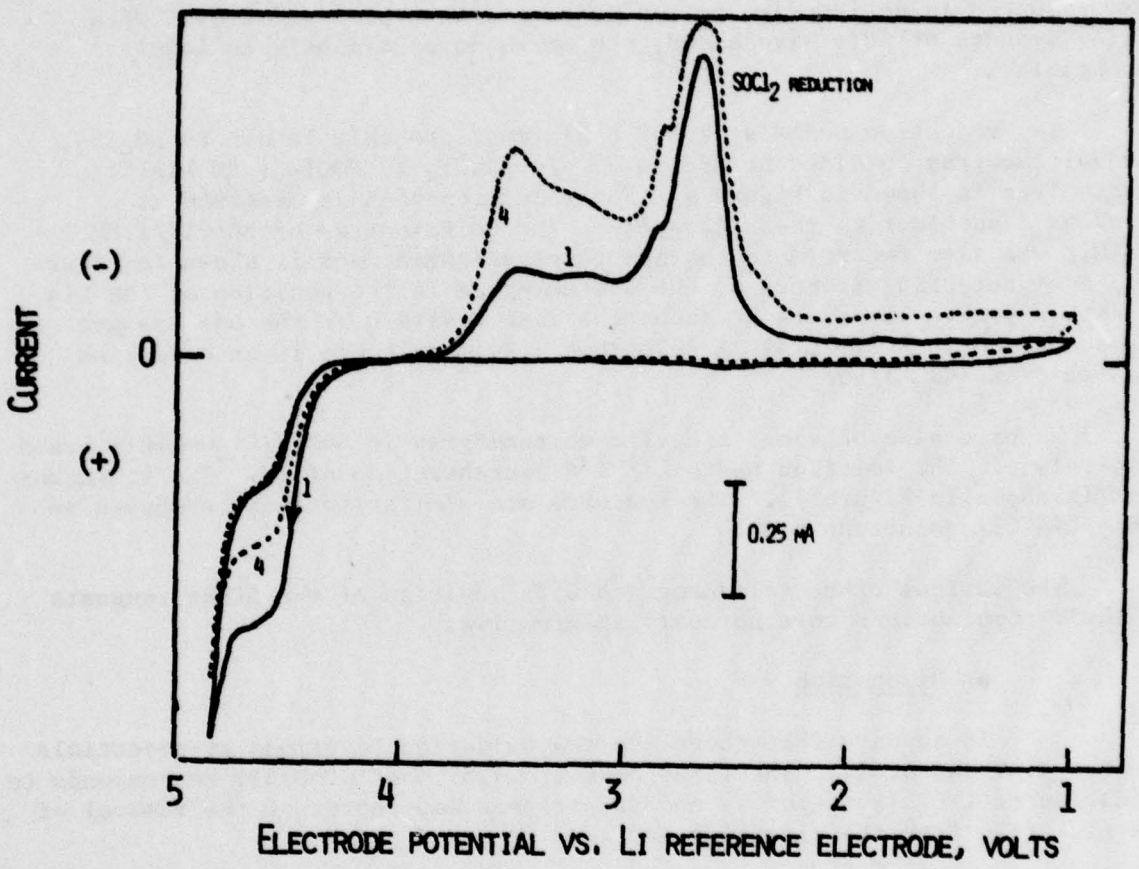

Fig. 7. Cyclic voltammogram of $SOCl_2$/1.8M $LiAlCl_4$ on a glassy carbon electrode. Scan rate = 100 mV/sec. The electrode was scanned anodic first from 3.7V. Cathodic curve 1 was obtained after voltage reversal at ∿4.9V. Curve 4 was obtained after twice cycling the electrode between 4 and 5V.

The voltammogram obtained by adding 1% SCl_2 to $SOCl_2$/1.8M $LiAlCl_4$ solution is shown in Figure 8. The onset of the cathodic current begins at 3.8V as in the case of the voltammogram in Figure 7. Addition of more SCl_2 resulted in an increase in the current with a peak at ∿3.6V. When larger amounts of SCl_2 were added, the peaks moved slightly to lower potentials.

The reduction peaks at 2.85V could most probably be due to SO_2Cl_2. The voltammogram obtained by adding 30 v/o SO_2Cl_2 to $SOCl_2$/1.8M $LiAlCl_4$ electrolyte is shown in Figure 9. The reduction peak is observed at ∿2.9V as a shoulder to the $SOCl_2$ peak. The voltammogram of SO_2Cl_2/1.8M $LiAlCl_4$ was also recorded to confirm this assignment and is shown in Figure 10. An interesting feature of the voltammogram is the position of the Cl_2 reduction peak. It occurs at about the same position as the one assigned to Cl_2 reduction in $SOCl_2$/$LiAlCl_4$ solutions. Evidently Cl_2 is an oxidation product of SO_2Cl_2 also.

We have also obtained a cyclic voltammogram in $SOCl_2$/Li_2O-$AlCl_3$ based electrolyte. The solution had a Li^+ ion concentration of 1M. The voltammogram is shown in Figure 11. The features are similar to those observed in $SOCl_2$/$LiAlCl_4$ solutions also.

The various other voltammograms with addition of the other reagents or their combinations were not very informative.

- Discussion

It appears that there are two oxidation reactions at potentials between 4.4V and 4.65V. The first peak at ∿4.5V most probably corresponds to oxidation of LiCl (Equation 2) and the process may represent the removal of the LiCl film from the electrode surface.

$$LiCl \rightarrow Li^+ + \frac{1}{2}Cl_2 + e^- \qquad (2)$$

The fact that it was possible to regenerate the electrode surface which had been passivated by holding it at a potential of ∿4.5V substantiate the assignment. The observed increase in the height of the peak after a cathodic sweep to 1V and the continuous decrease in the height of the peak on successive cycling between 4V and 5V are also in agreement for this assignment.

The more positive broad peak at 4.65V may correspond to the oxidation of $AlCl_4^-$, (Equation 3).

$$AlCl_4^- \rightarrow \frac{1}{2}Cl_2 + AlCl_3 + e^- \qquad (3)$$

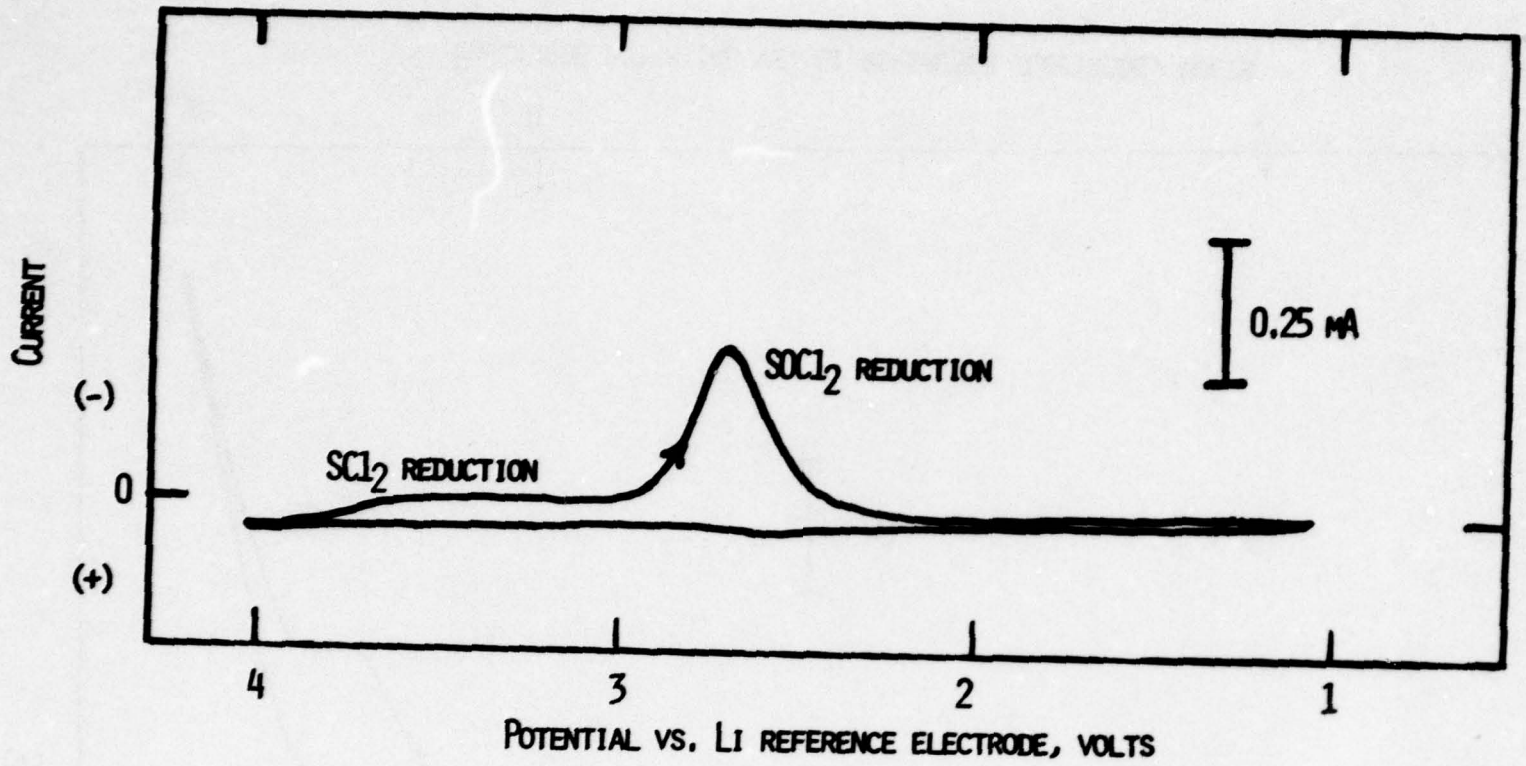

Fig. 8. Cyclic voltammogram of $SOCl_2$/1.8M $LiAlCl_4$ with 1.5 v/o SCl_2 on glassy carbon. Scan rate = 50 mV/sec. Cathodic scan first.

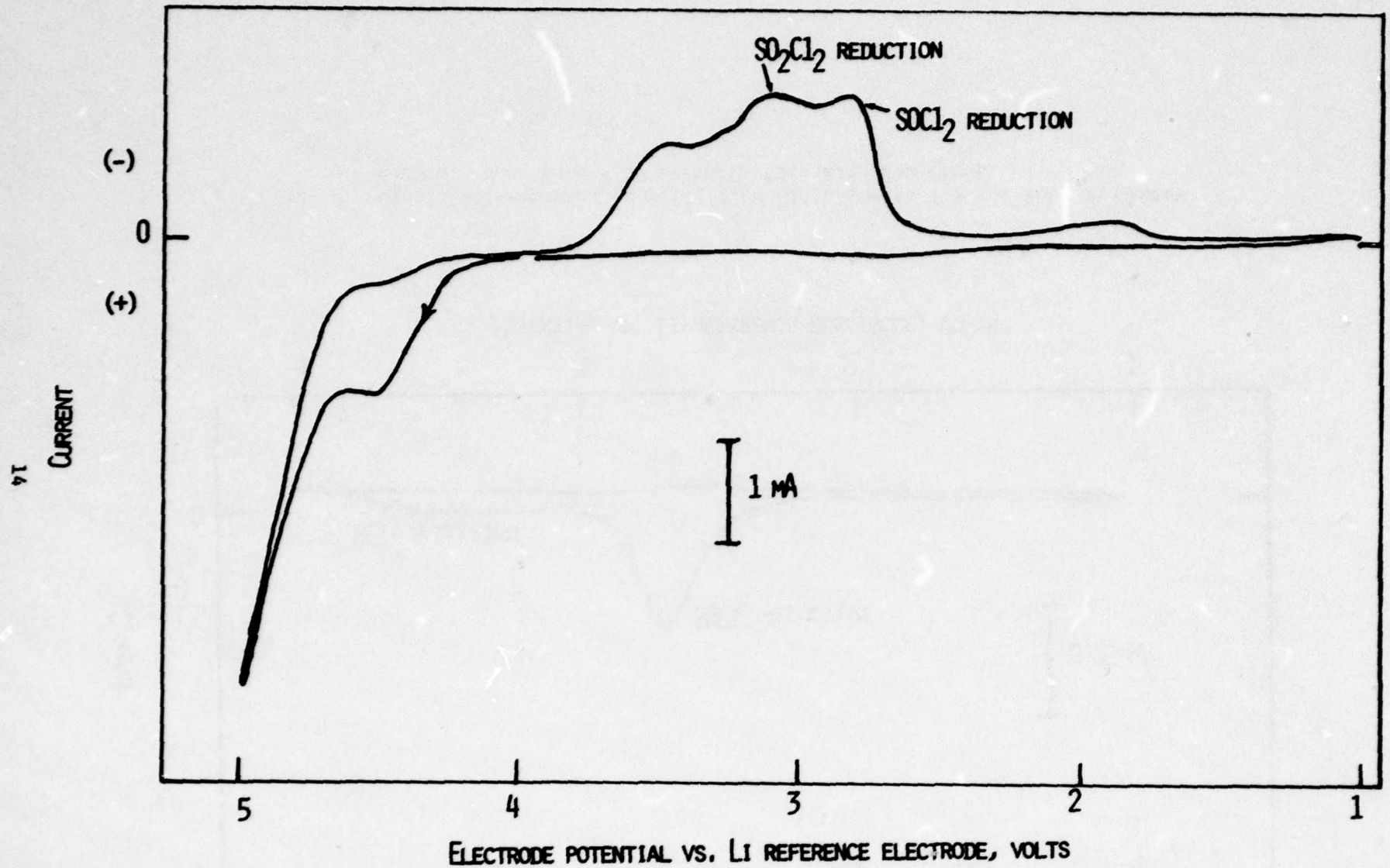

Fig. 9. Cyclic voltammogram of $SOCl_2$/1.8M $LiAlCl_4$ containing 30 v/o SO_2Cl_2 on glassy carbon electrode. Anodic scan first. Scan rate = 50 mV/sec.

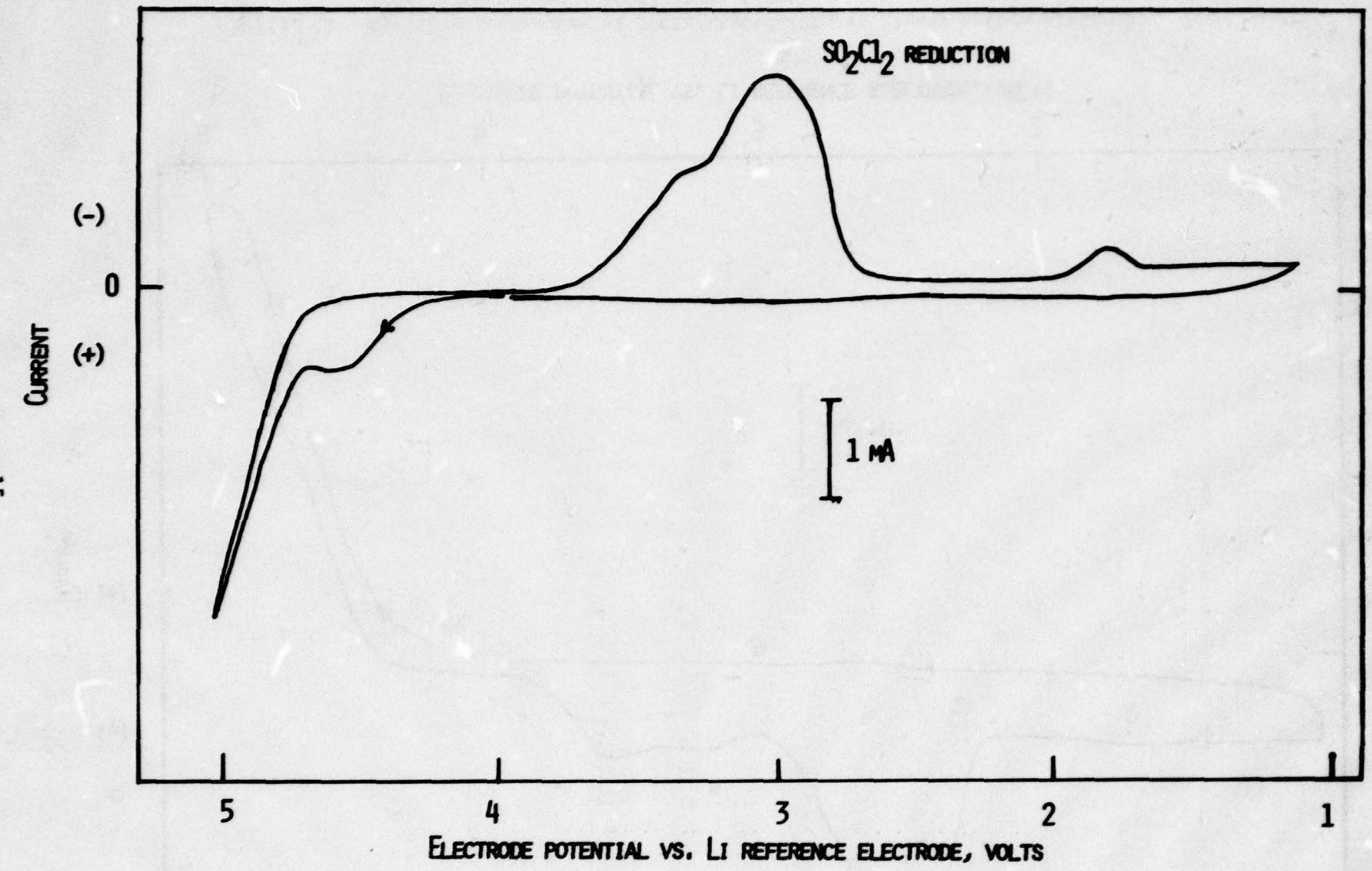

Fig. 10. Cyclic voltammogram of SO_2Cl_2/1.8M $LiAlCl_4$ on glassy carbon electrode between 1 and 5 volts. Scan rate = 50 mV/sec. The electrode was scanned anodic first.

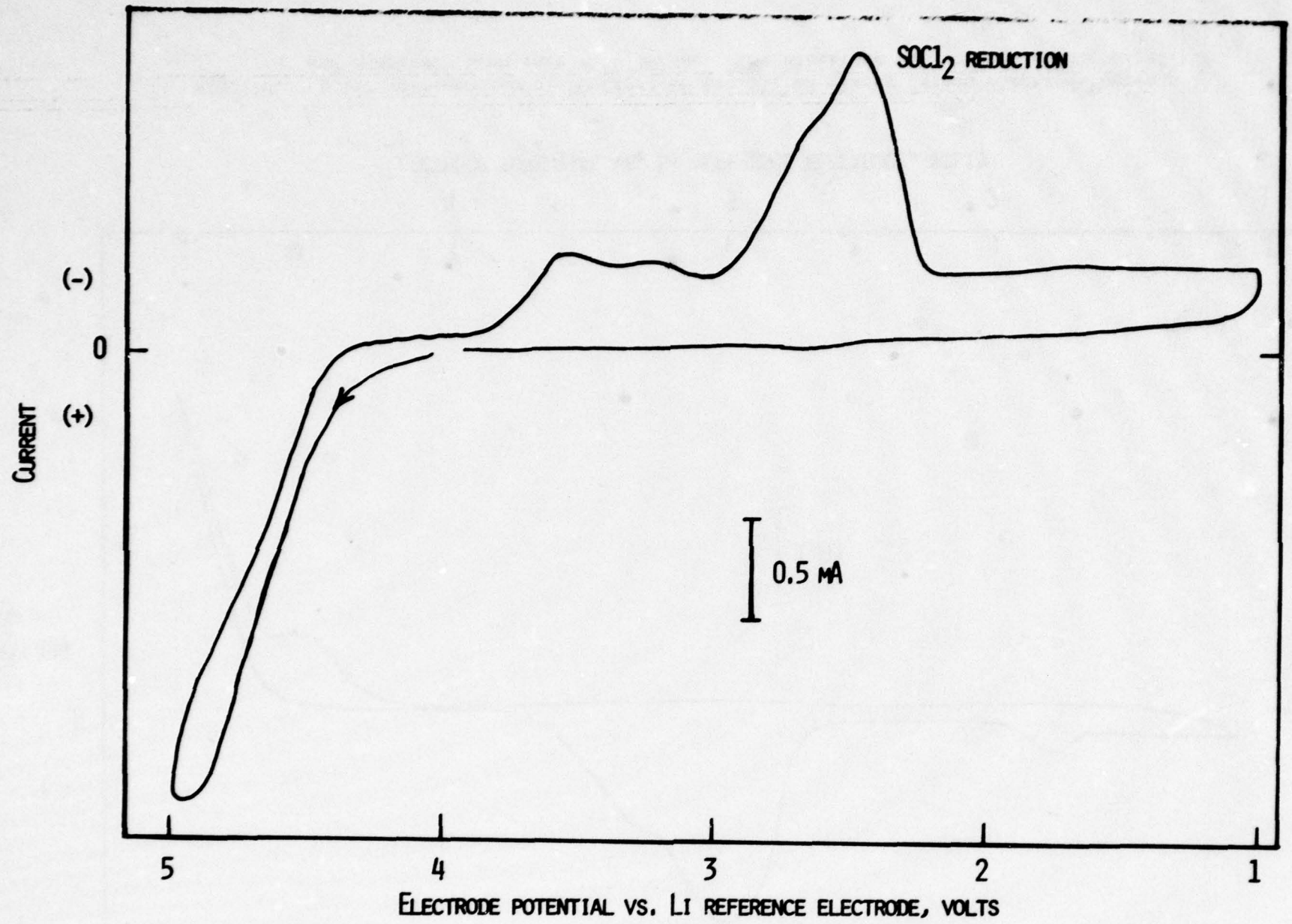

Fig. 11. Cyclic voltammogram of $SOCl_2/Li_2O$-$2AlCl_3$ on glassy carbon electrode. Scan rate = 200 mV/sec. Anodic scan first.

When the voltammograms were run in $SOCl_2/LiAlCl_4$ solutions as a function of the concentration of $LiAlCl_4$ from 0.25 to 2.0M, we found increasing peak heights with increasing concentration of $LiAlCl_4$. The results from these experiments are not conclusive. However, we had identified (10,11) $AlCl_3$ as an oxidation product of $SOCl_2/LiAlCl_4$ solution when these solutions were electrolyzed at constant current with the anode potential remaining at ∿4.6V.

The high current peak near 5V is most probably due to oxidation of $SOCl_2$. However, the oxidation may begin at a much lower potential; say, at ∿4.6V in keeping with the fact that products of $SOCl_2$ were present (10,11) in the $SOCl_2/LiAlCl_4$ electrolyte after constant current electrolysis at anode potentials of 4.6V.

The predominant reactions at 4.6V could then be reaction (2) and reactions (3) and (4) shown below.

$$AlCl_4^- \rightarrow AlCl_3 + \tfrac{1}{2}Cl_2 + e^- \qquad (3)$$

$$SOCl_2 + AlCl_4^- \rightarrow SOCl^+AlCl_4^- + \tfrac{1}{2}Cl_2 + e^- \qquad (4)$$

Reaction (2) would occur predominantly only if the electrode had been first scanned cathodically from open circuit so as to cause LiCl deposition on the electrode by $SOCl_2$ reduction. Reaction 4 is now accepted as the primary oxidation process in $SOCl_2/LiAlCl_4$ solutions (7,11).

A further discussion of the oxidation products of $SOCl_2$ may be made with reference to the voltammogram below 4V obtained by sweeping the electrode cathodically after an anodic scan to 5V (see Fig. 7).

Since the anodic peak at 4.6V and the cathodic peak at 3.25V are interdependent, and since the primary reactions at 4.6V involve the formation of Cl_2, the peak at 3.25V is most probably due to Cl_2 reduction. This assignment is supported by the observation that a solution of Cl_2 in $SOCl_2/LiAlCl_4$ shows a reduction peak at 3.25V and that the Cl_2 reduction peak in $SO_2Cl_2/LiAlCl_4$ is formed at ∿3.25V.

The reduction peak at 3.6V can be assigned tentatively to a sulfur chloride such as SCl_2 with reference to the voltammogram in Figure 8. The reduction potential observed here for SCl_2 is in agreement with the value reported by Blomgren et al. (8). They found that SCl_2 reduces at ∿3.7V vs. Li^+/Li in $SOCl_2$. Two other experimental results also suggested that the peak at ∿3.6V is most probably due to SCl_2. In $SOCl_2/LiAlCl_4$ solutions containing S or S_2Cl_2, the reduction peaks at 3.6V showed higher currents than in solutions without the additives, suggesting that these materials may chemically

react with an anodic product to give the material with the 3.6V reduction potential. Since Cl_2 is an oxidation product, the most probable reactions are,

$$S_2Cl_2 + Cl_2 \rightarrow 2SCl_2 \quad (5)$$

$$S + Cl_2 \rightarrow SCl_2 \quad (6)$$

These reactions are well known. For example SCl_2 is prepared by passing dry Cl_2 gas through powdered S. The reaction is exothermic and the intermediate is S_2Cl_2. In this reaction, with a large excess of Cl_2, the unstable SCl_4 can also be prepared by proper low temperature cooling.

From these information we assign the reduction peak at 3.6V as most probably due to SCl_2. However SCl_2 is a reduced S species and its formation on oxidation of $SOCl_2/LiAlCl_4$ is somewhat unusual. Nevertheless, a reaction mechanism involving the formation of SCl_2 can be written for oxidation reactions in $SOCl_2/LiAlCl_4$ which could account for all the products:

The reduction peak at 2.85V may correspond to SO_2Cl_2 in accordance to the results presented in Figures 9 and 10.

Oxidation reactions that would explain the formation of the various products observed here could then be, (2), (3), (4) and (7) and (8) shown below.

$$SOCl_2 + SOCl^+AlCl_4^- \rightarrow SCl^+ + AlCl_3 + \tfrac{1}{2}Cl_2 + e^- + SO_2Cl_2 \quad (7)$$

$$SCl^+ + AlCl_4^- \rightarrow SCl^+AlCl_4^- \quad (8)$$

The cathodic processes to balance the charges would involve the reduction of $SOCl_2$ with Li^+ from $LiAlCl_4$ as shown in Equation (1).

The first oxidation reaction of $SOCl_2$ shown in Equation (4) is now well accepted. However, we note that $SOCl^+AlCl_4^-$ is structurally similar to $LiAlCl_4$ and could be oxidized at potentials close to that of the oxidation of $LiAlCl_4$. Although the reactions in (7) and (8) may represent the overall processes, the actual reactions may take place in multisteps as shown in (9) and (10).

$$2SOCl^+AlCl_4^- \rightarrow 2AlCl_3 + ClO_2 + 2e^- + \tfrac{1}{2}Cl_2 + 2SCl^+ \quad (9)$$

$$2SOCl_2 + ClO_2 \rightarrow 2SO_2Cl_2 + \tfrac{1}{2}Cl_2 \quad (10)$$

Note that this reaction scheme involves a very explosive and powerful oxidizing agent ClO_2. The complex $SCl^+AlCl_4^-$ is essentially $AlCl_3$ complex of SCl_2 and has been previously characterized (12).

We would like to stress that the reaction schemes shown above have been proposed to explain the observed products. More work is needed for further confirmation.

III. ANALYSIS OF ELECTROLYTE FROM Li/$SOCl_2$ CELLS AFTER DISCHARGE, FORCED OVERDISCHARGE AND "CHARGE"

A preliminary account of the analysis of products from discharged and overdischarged Li/$SOCl_2$ cells by IR spectrometry was given in the last quarterly report. Further studies were made in the present quarter using both IR spectrometry and *in situ* cycle voltammetry. The small prismatic cells with a slightly flooded configuration was used for these studies. The larger amounts of electrolyte were needed to have materials left for analysis after the galvanostatic tests. Control experiments with extracts of the electrode package from cells containing lesser amounts of electrolyte did not show results different from flooded cells.

1. Experimental Procedure

In the IR spectrometric methods anode and cathode limited cells were subjected to various states of discharge and overdischarge and the electrolyte was analyzed. The electrode package was then extracted with $SOCl_2$ on SCl_2 and spectra were again recorded. In order to identify the spectra, spectra of mixtures of various reagents of known compositions were also obtained.

All infrared spectra were obtained on a Beckman Acculab 5 dual beam spectrometer. The instrument covers the range 4000 cm^{-1} to 375 cm^{-1}. All the liquid spectra were obtained with Beckman TAC cells. These have AgCl windows of 0.025 to 0.1 mm path length and can be sealed permanently.

The IR data were complemented by cyclic voltammetry studies. Attempts to obtain cyclic voltammetry data with a microcarbon electrode incorporated inside the cell between two layers of the electrode package were not successful due to passivation from excessive film formation on the electrode surface. However, informative results were obtained from cyclic voltammetry on a glassy carbon microelectrode (0.07 cm^2) introduced into the cell through a side arm of the specially designed glass cell. The cell and the electrode arrangement is shown schematically in Figure 12. During discharge the microcarbon electrode was removed from the electrolyte. In order to record the voltammogram after discharge and overdischarge, the electrode was pushed down and secured contact with the electrolyte by placing the cell in a tilted position. Passivation of the electrode was avoided by this procedure. Reproducible results were obtained. The cell reference electrode and Li electrode were used as the reference and counter electrodes for CV.

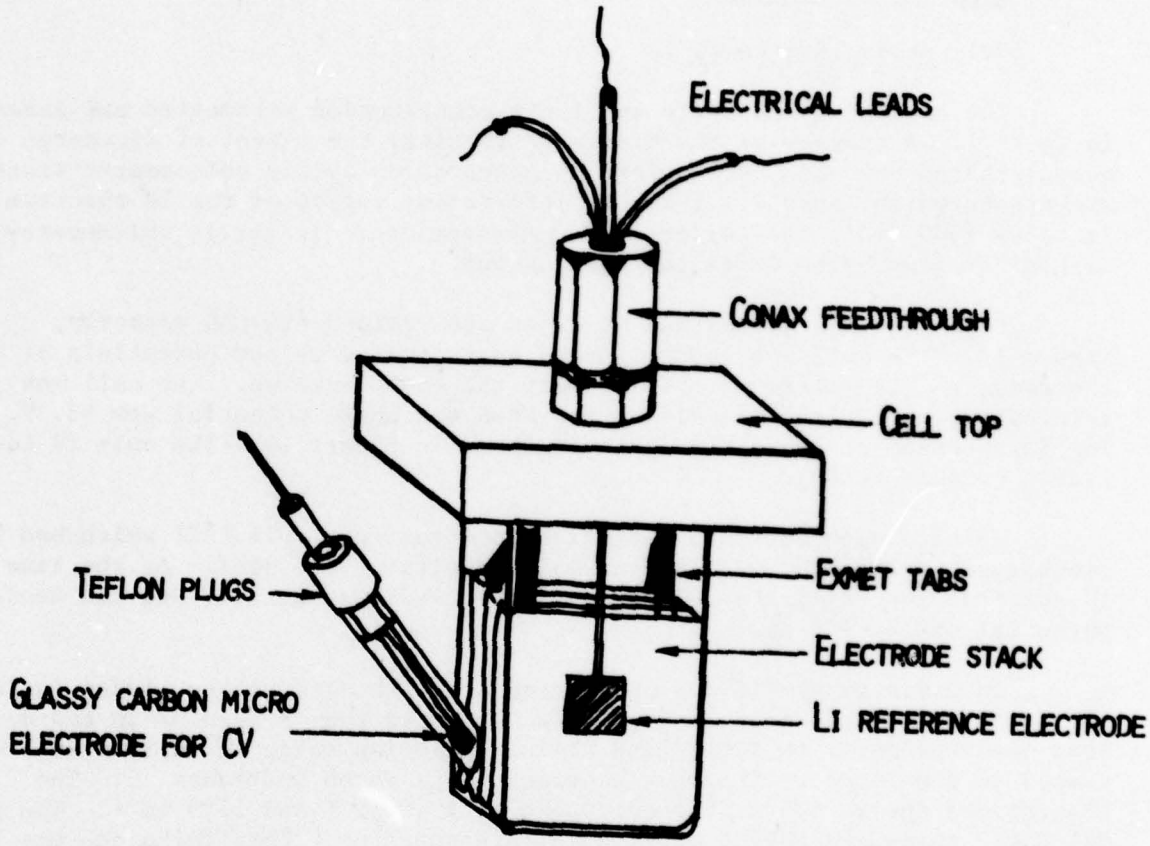

Fig. 12. Schematic view of the cell for in situ cyclic voltammetry.

Since the IR spectral data and cyclic voltammetry results are complementary, it is appropriate to discuss the data with respect to cell configurations and the modes of cell operation.

2. Experimental Results

2.1 Anode Limited Cells

The anode limited cells and their construction parameters are given in Table 1. A summary of the discharge results, the extent of discharge or overdischarge for each cell before IR spectral or cyclic voltammetry tests are presented in Table 2. The most informative region of the IR spectrum is below 1500 cm^{-1}, the region of S-O absorptions. In cyclic voltammetry, the cathodic region below 4V is the most useful.

Cell P-22 was discharged at 27 mA and yielded 490 mAh capacity, Figure 13. The cell was anode limited as indicated by the potentials of the anode vs. Li reference electrode at the end discharge. The cell was terminated just at the end discharged when the anode potential was ∿3.5V. The IR spectrum of the electrolyte is shown in Figure 14. The only IR identifiable product is SO_2.

We have also obtained a similar spectrum from cell P-21 which had been discharged to 260 mAh, ∿2/3 the normal capacity of the cell. At the time of IR spectral recording the cell potential in P-21 was at 3.4V and the anode potential was at +50 mV.

In order to see if any other products with absorptions hidden inside the large $SOCl_2$ peak near 1200 cm^{-1}, we recorded the IR spectra in the double beam spectrometer with $SOCl_2$/1.8M $LiAlCl_2$ solution taken in an identical cell placed in the reference beam. The spectrum is shown in Figure 15. The absorptions due to SO_2 are clearly seen at 1340 cm^{-1} and 1155 cm^{-1}. The normal $SOCl_2$ peaks are folded upwards in this spectrum. This technique was found to be a useful one of general utility in the IR spectral studies of this system.

Another anode limited cell P-18 was discharged at 24 mA and then forced overdischarged also at 24 mA. The overdischarge proceeded with considerable voltage fluctuations as often found (10,11) in anode limited cells during forced overdischarge. The discharge and overdischarge are presented in Figure 16. The IR spectrum was recorded after 240 mAh of overdischarge and is shown in Figure 17. The spectrum shows SO_2 as the major product. However, another new peak of medium intensity is present at 1070 cm^{-1}. The spectrum obtained with $SOCl_2/LiAlCl_4$ solution in the reference beam showed that no material is present which absorbs at 1200 cm^{-1}. The IR spectrum from anode limited cell P-26 (Figure 18) overdischarged for 1.1 Ah was identical to the one in Figure 19 except that the intensity of the peak at 1070 cm^{-1} was relatively higher. We have reproduced this result in yet another cell overdischarged for 2Ah.

Table 1

Cell Parameters for Anode Limited Cells

Cell No.	Cell Configuration	Carbon Electrode			Lithium Electrode		Electrolyte $LiAlCl_4/SOCl_2$		
		Average Thickness (mm)	Total Area Facing Li (cm^2)	Approximate Amount of Carbon (mg)	Area (cm^2)	Amount (Ah)	Con. $LiAlCl_4$ (M)	Vol. (ml)	Discharge Current (mA)
P-18	C/Li/C/Li/C (AL*)	0.65	24	400	24	0.63	1.8	4.5	24
P-19	AL, without Li on the anode Exmet	0.75	24	530	-	-	1.8	4.0	24
P-21	AL	0.75	24	470	24	0.63	1.8	4.0	24
P-22	AL	0.75	24	450	24	0.63	1.8	4.0	27
P-23	AL, without Li on the anode Exmet	0.70	24	450	-	-	1.8	4.0	50
P-26	AL	0.68	24	480	24	0.63	1.8	3.5	24
P-31	AL, no lithium	0.68	24	400	-	-	1.8	4.0	24
P-32	AL	0.69	24	400	24	0.63	1.8	4.0	24

*AL → anode limited.

Table 2

Analytical Test Summary of Anode Limited Cells

Cell No.	Cell Capacity (mAh)	Test Performed After: Discharge, mAh IR	Discharge, mAh CV	Overdischarge, mAh IR	Overdischarge, mAh CV
P-18	396			240	
P-19	Cell without Li			670	
P-21	260*	260*			
P-22	490	490			
P-23	Cell without Li			1150	
P-26	620			1100	
P-31	Cell without Li			3300	3300
P-32	490		490	2160	2600

*Partial discharge.

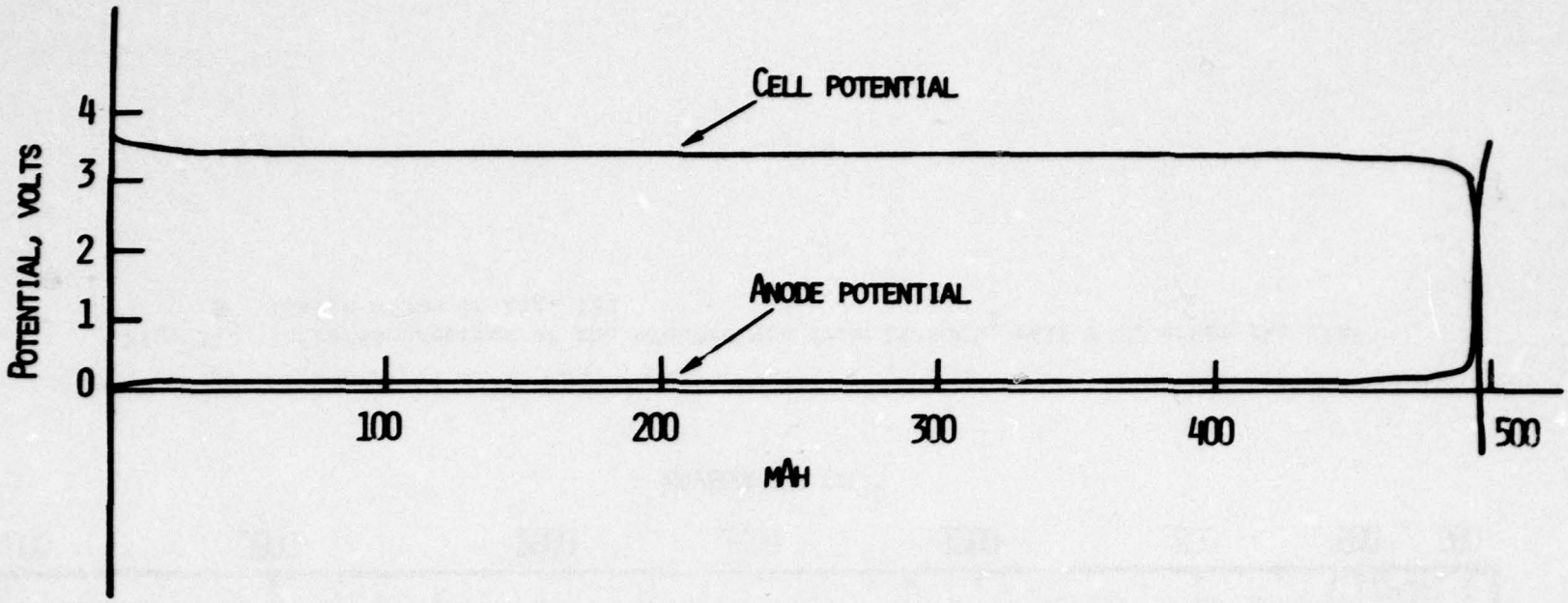

Fig. 13. Discharge curve for $Li/SOCl_2$ cell P-22. Current = 24 mA.

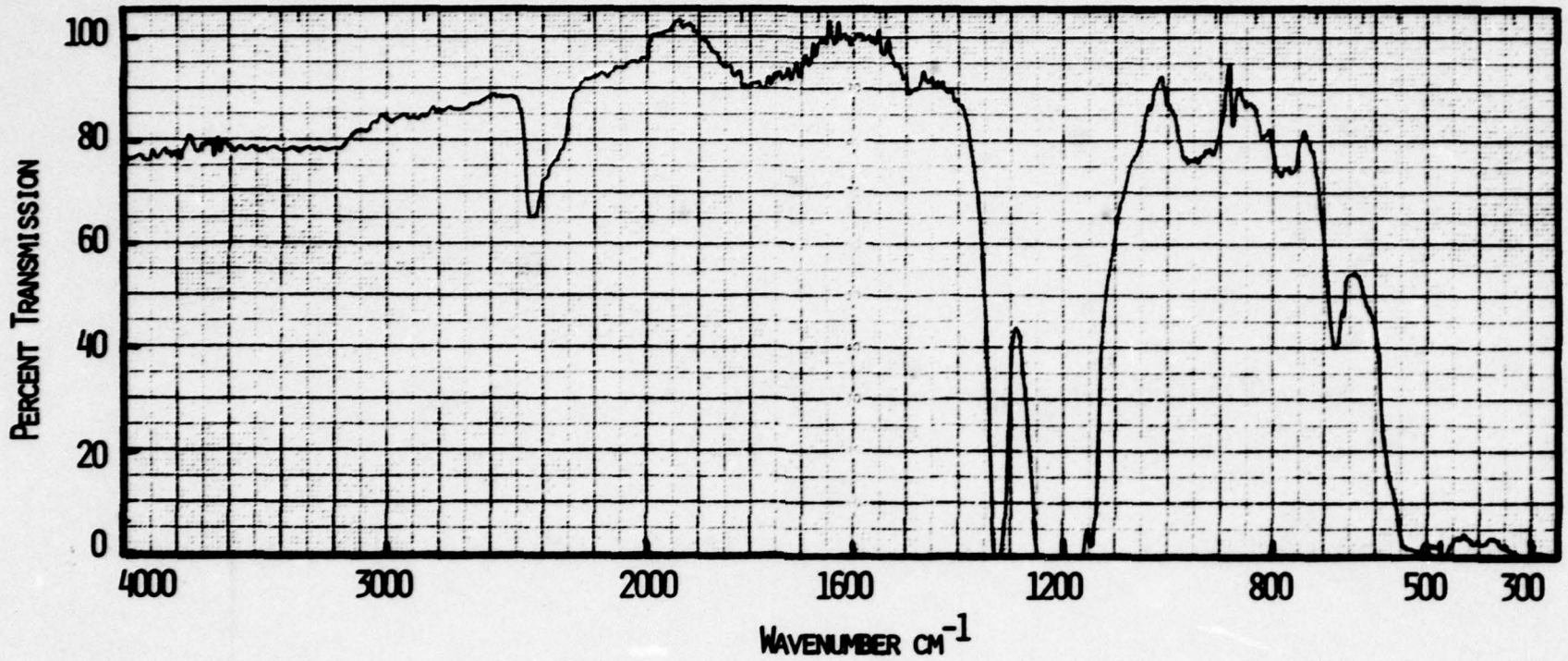

Fig. 14. Infrared spectrum of the electrolyte from Li/$SOCl_2$ cell P-22 after the discharge shown in Fig. 13.

Fig. 15. Infrared spectrum of electrolyte from Li/$SOCl_2$ cell P-22 after 0.49 mAh discharge shown in Fig. 13. The reference cell contained $SOCl_2$.

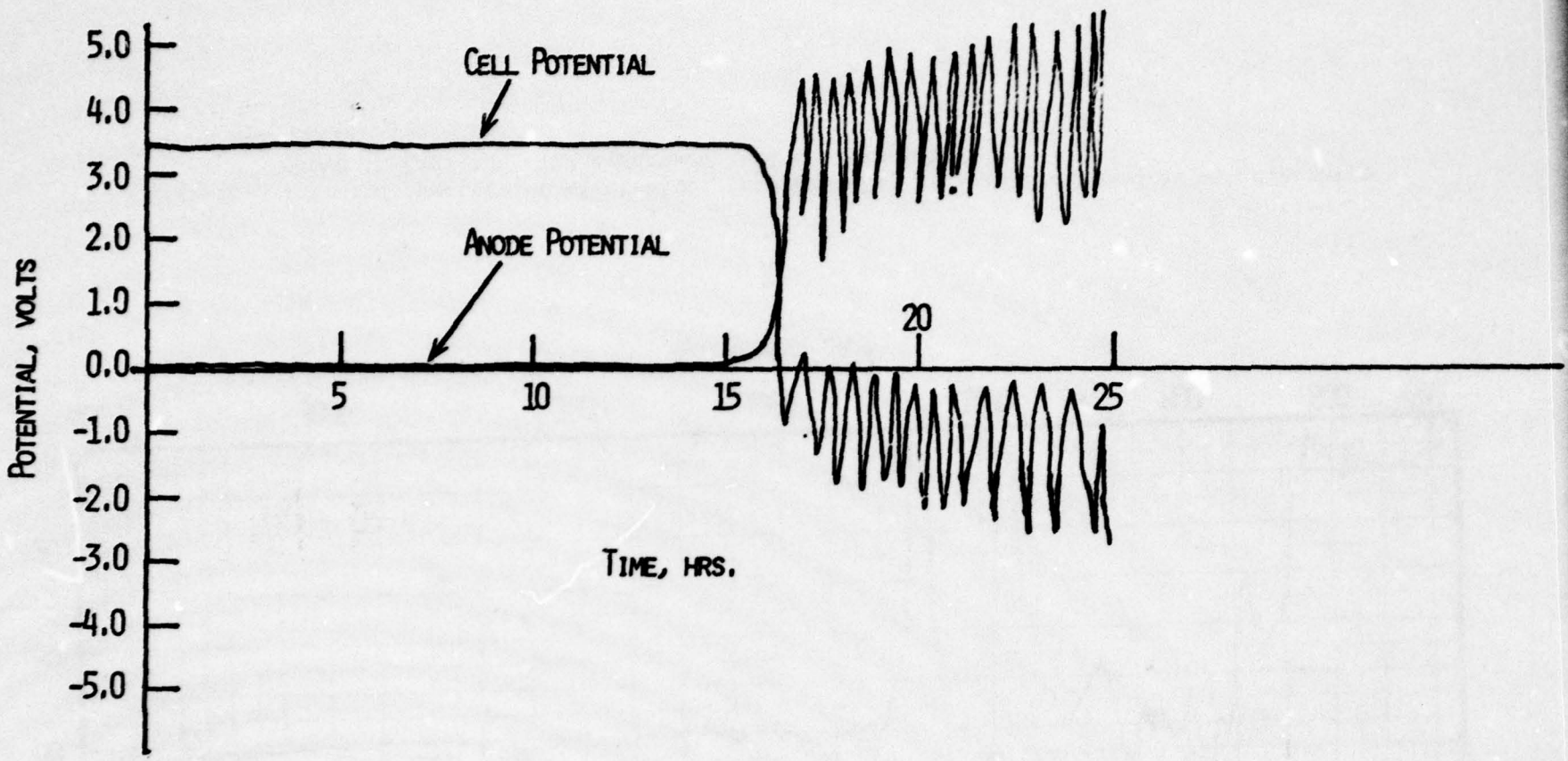

Fig. 16. Galvanostatic discharge and overdischarge curves for Li/$SOCl_2$ cell P-18. Current = 24 mA.

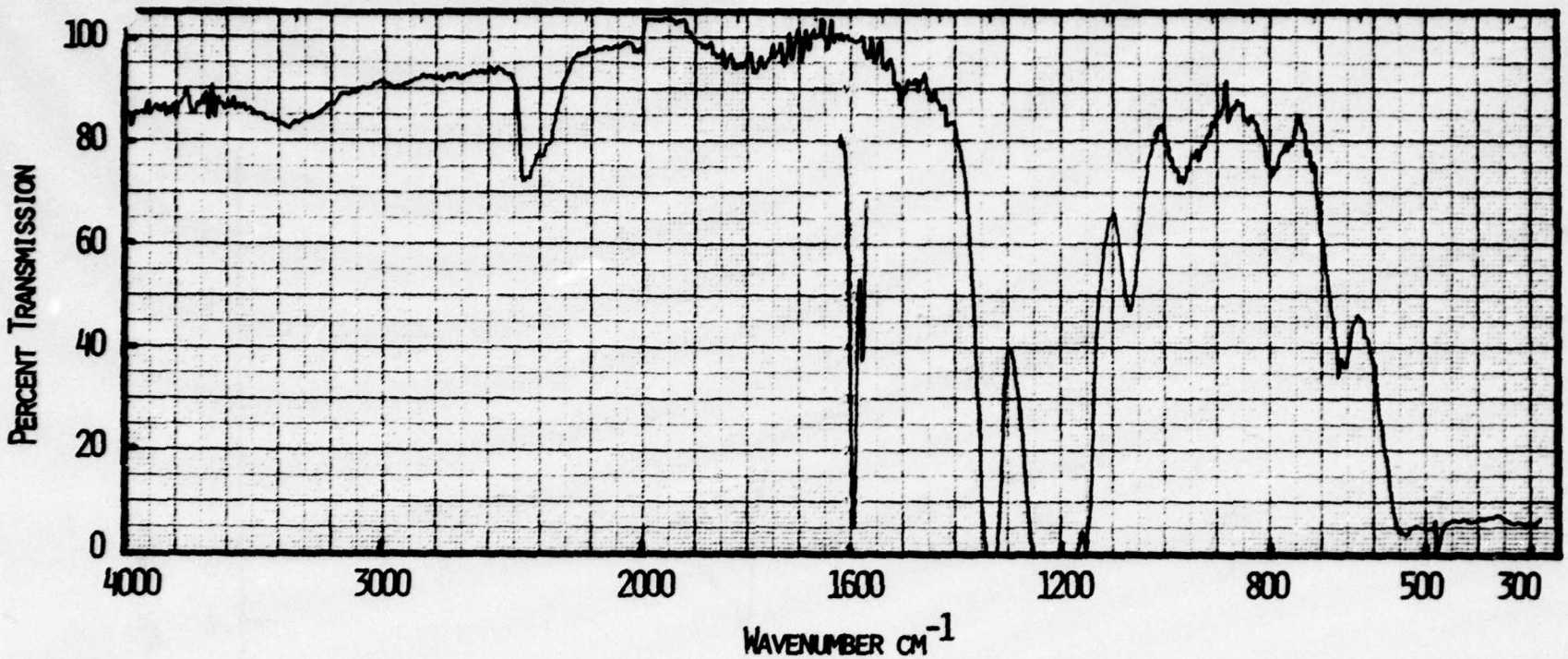

Fig. 17. Infrared spectrum of electrolyte from Li/$SOCl_2$ cell P-18 after the overdischarge shown in Fig. 16.

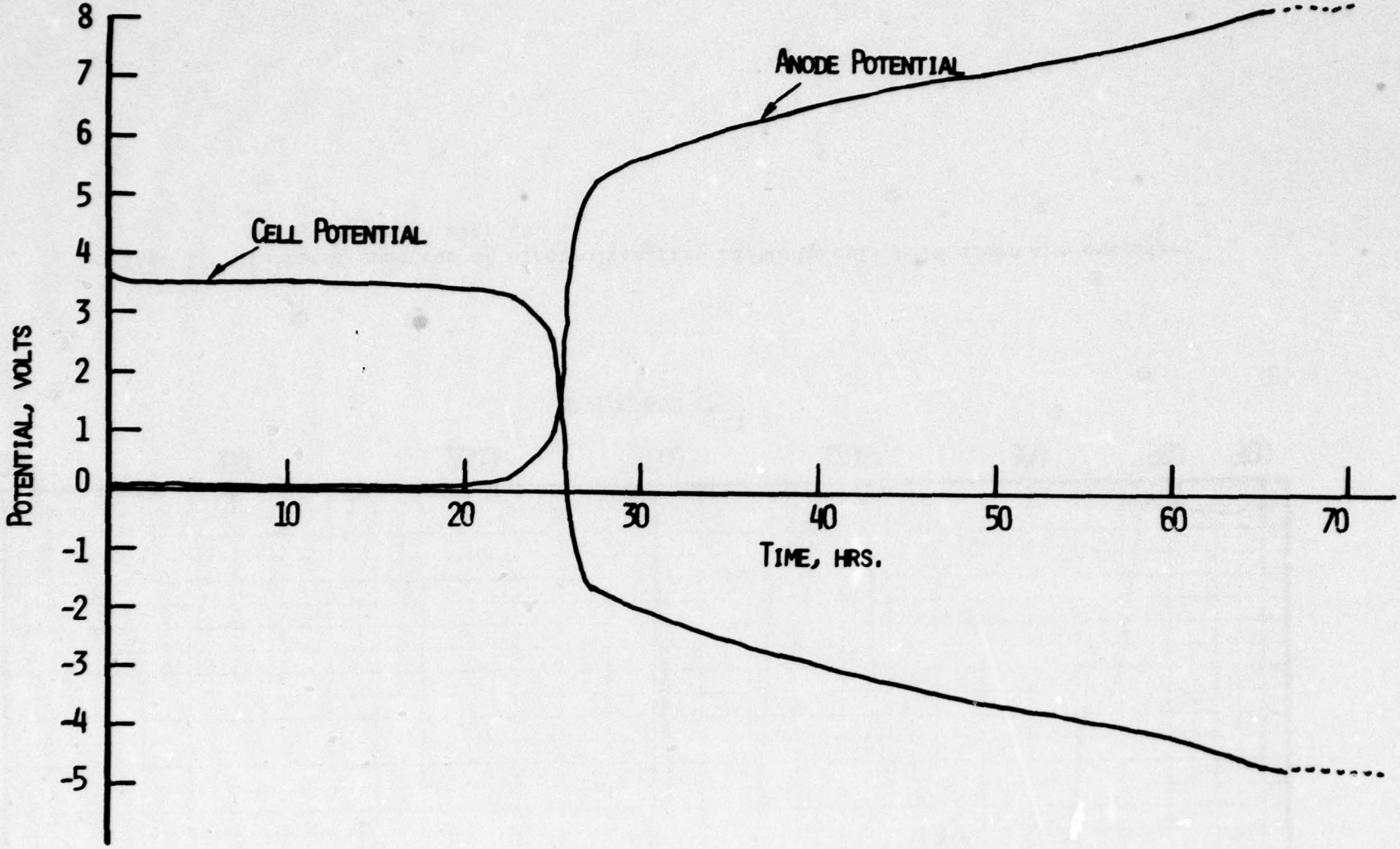

Fig. 18. Discharge and overdischarge curves for Li/$SOCl_2$ cell P-26. Current = 24 mA.

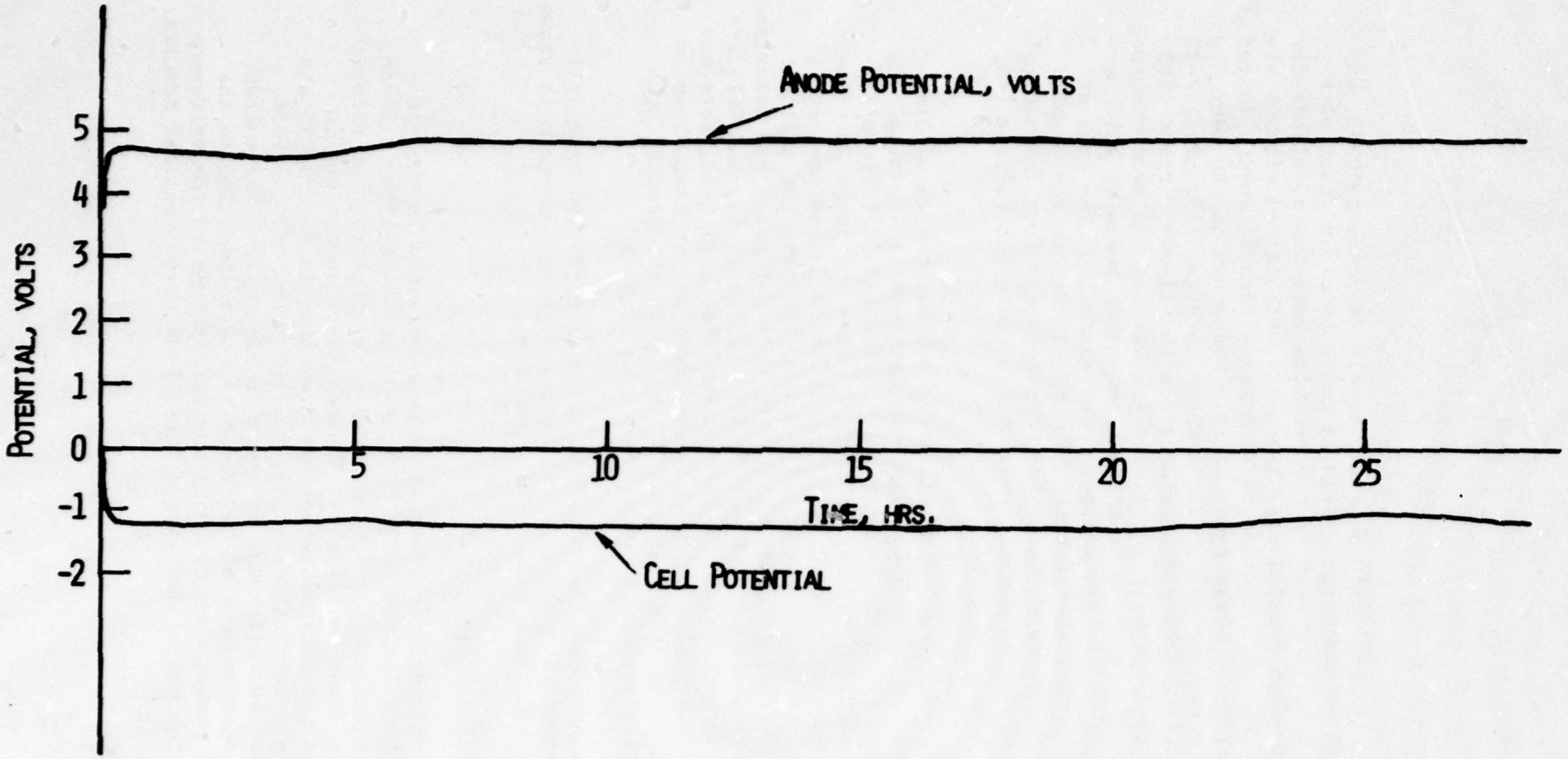

Fig. 19. Discharge curve for cell P-19 without Li on the anode. Current = 24 mA.

In all the anode limited cells some Li, mostly in loose patches, was still present at the end of discharge. This Li could possibly react with the oxidation product(s) so that some of the products were not available for detection. To eliminate this possibility, two cells were tested without any lithium on the anode. This cell represents an extreme case of anode limited cell, the discharge profile of these types of cell was shown in the last report. The discharge curve for cell P-19 is shown in Figure 19. Cell P-23 was tested without the Li reference electrode since the Li could react with oxidation products. Both cells gave identical IR spectra. The spectrum from P-19 is shown in Figure 20. The spectrum shows two other peaks at 1410 cm^{-1} and 1110 cm^{-1} in addition to the peaks present in Figure 17. The peak at 1410 cm^{-1} is due to SO_2Cl_2 and the peak at 1110 cm^{-1} is due to the complex $SOCl^+AlCl_4^-$. These compounds were characterized previously from IR spectral data in solutions of $SOCl_2/LiAlCl_4$ after constant current electrolysis (10, 11).

Cyclic voltammetry data were obtained after various stages of discharge and overdischarge. A typical voltammogram obtained by scanning the C electrode between 1 and 4V in the electrolyte from cell P-32 (Figure 21) which had been forced overdischarge for 2.16 Ah is shown in Figure 22. The voltammogram shows a reduction peak at 3.25V due to an oxidation product. A very low current peak may be present at $\sim$3.6V. We note that the voltammogram obtained after 490 mAh of discharge when the anode potential had polarized to $\sim$4.0V did not show any peaks at 3.6V and 3.25V. Evidently Cl_2 and SCl_2 are present in the overdischarged cell. The IR spectrum from cell P-32, obtained immediately after the cyclic voltammetry run, was identical to that shown in Figure 19, showing principally the peak at 1070 cm^{-1} from the product. In addition, SO_2 and a minute amount of SO_2Cl_2 were also present.

A cyclic voltammogram was also obtained in the electrolyte from cell P-31, Figure 23, discharged without Li on the anode. The voltammogram is shown in Figure 24. It shows the peaks due to Cl_2, and SCl_2.

2.2 Cathode Limited Cells

Both IR spectra and cyclic voltammograms were obtained in the electrolytes from three cathode limited cells P-29, P-35 and P-36 after 3.24 Ah, 1.87 Ah and 1.08 Ah of overdischarge respectively. The construction parameters of these cells are shown in Table 3. The tests are summarized in Table 4. The discharges and overdischarges are presented in Figures 25 and 26 for cells P-35 and P-36 respectively. The voltammograms of cell P-36 obtained after 1.87 Ah of overdischarge is shown in Figure 27. The voltammogram shows a small reduction peak at 3.25V due to Cl_2 in addition to the $SOCl_2$ and SO_2 reduction peaks. The Cl_2 peak was not present in the voltammograms recorded just at the end of discharge. Cell P-36 gave identical results.

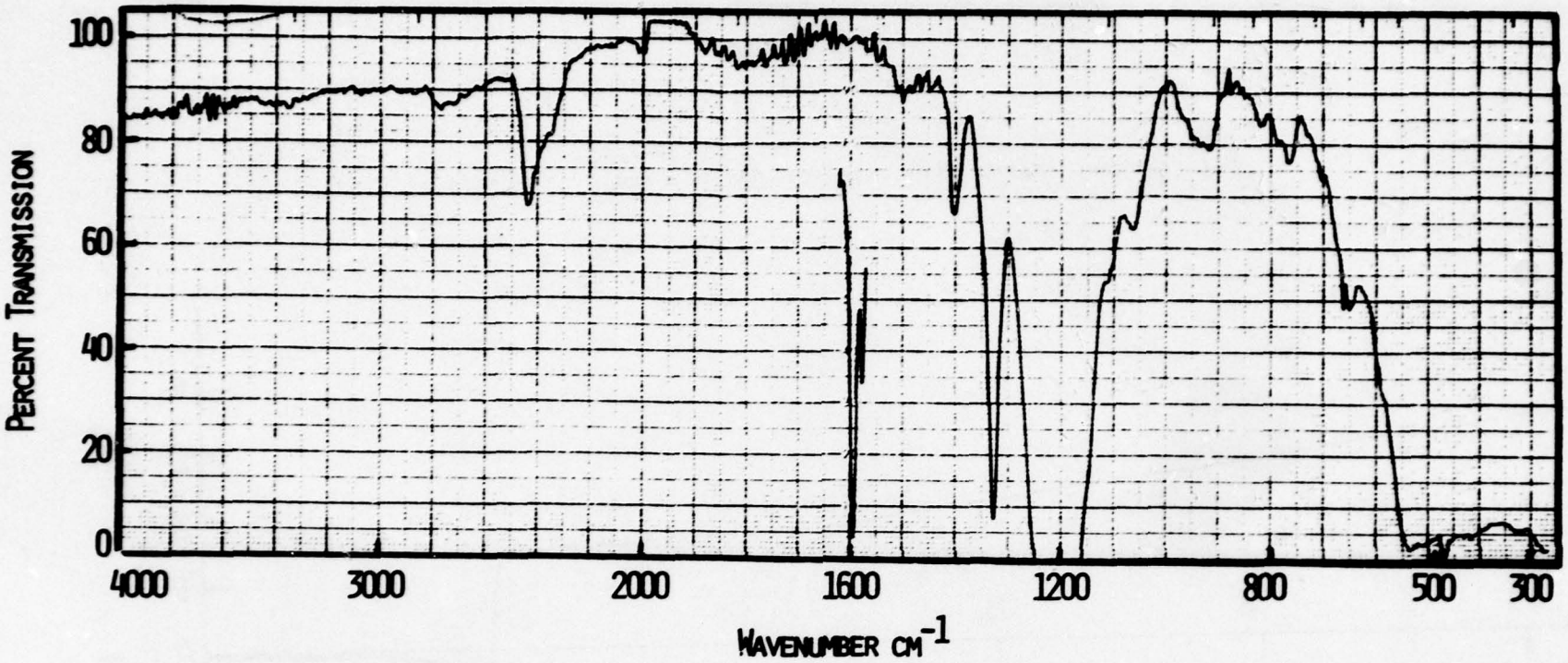

Fig. 20. Infrared spectrum of the electrolyte from cell P-19 shown in Fig. 19.

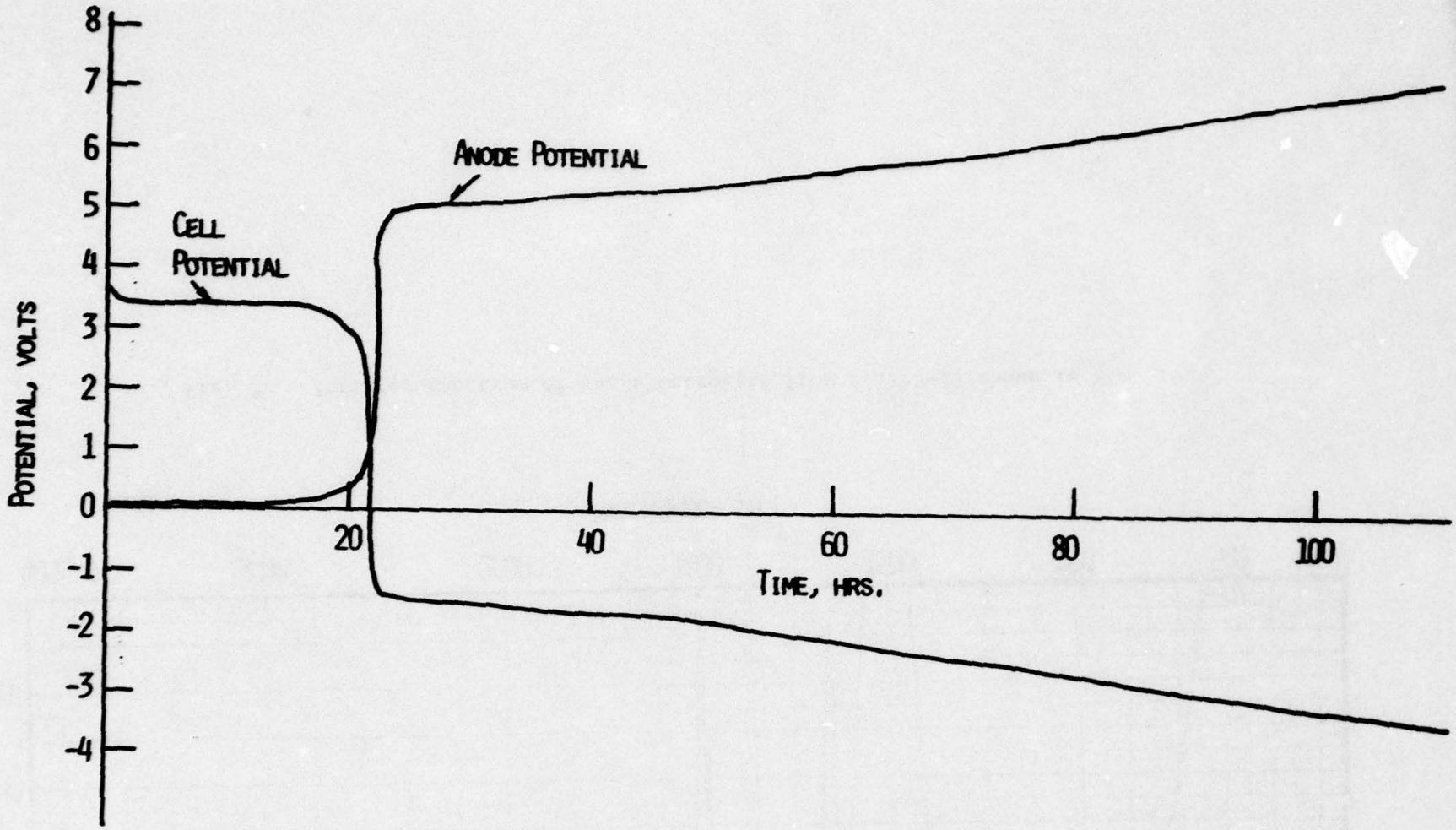

Fig. 21. Discharge and overdischarge curves for cell P-32. Current = 24 mA.

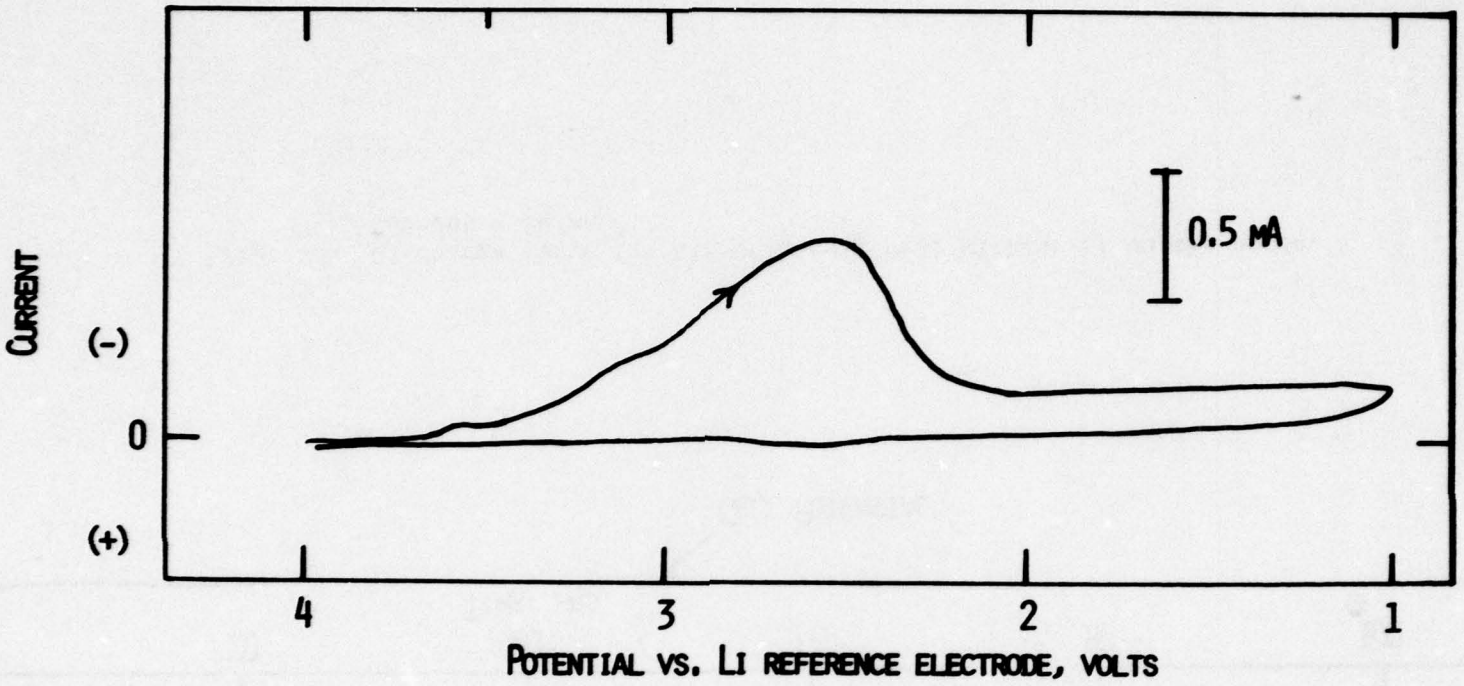

Fig. 22: Cyclic voltammogram of electrolyte from cell P-32 after 550 mAh overdischarge on glassy carbon electrode. Scan rate = 50 mV/sec. Cathodic scan first.

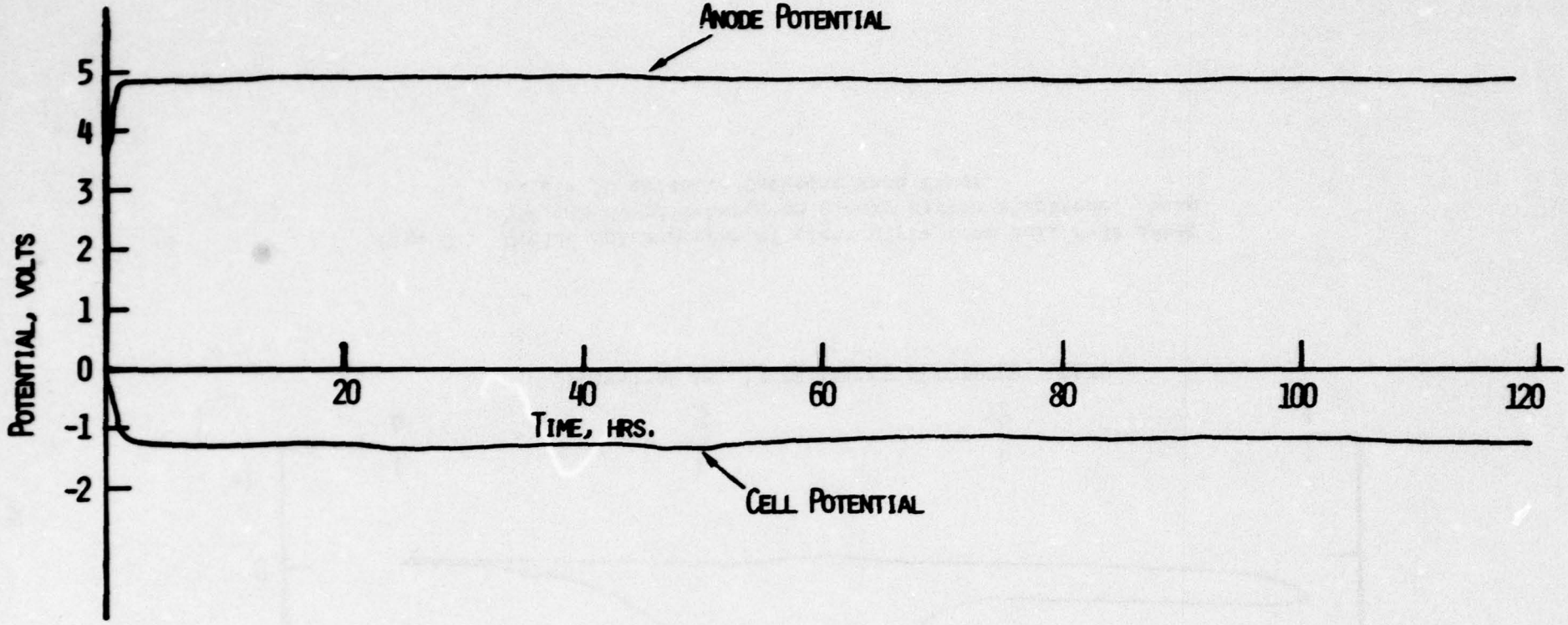

Fig. 23. Discharge curve for Li/$SOCl_2$ cell P-31 without Li on the anode. Current = 24 mA.

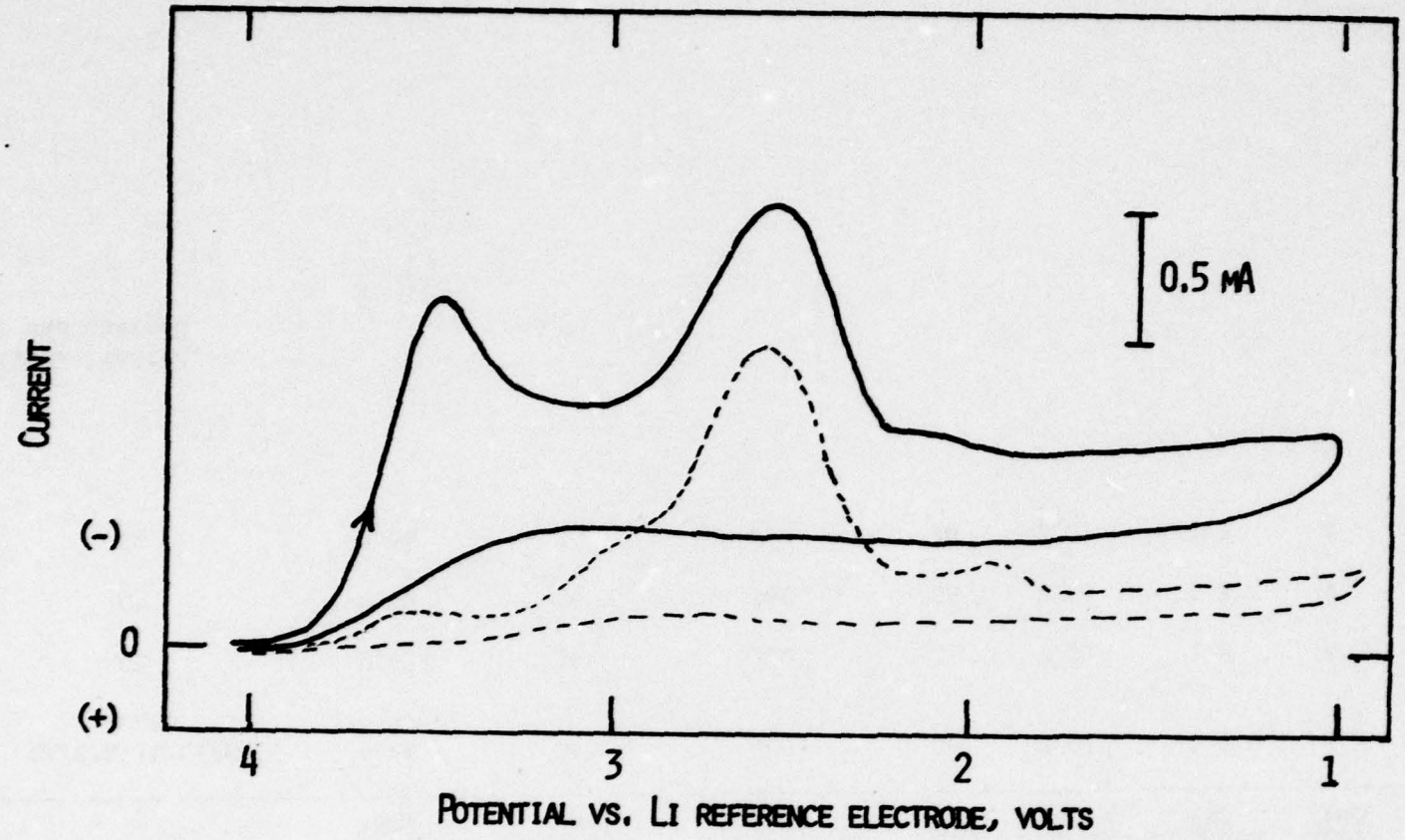

Fig. 24. Cyclic voltammogram of electrolyte from cell P-31 on glassy carbon electrode. The solid curve represents the voltammogram obtained after the discharge shown in Fig. 23. The voltammogram represented by the broken curve was obtained after 0.10 Ah discharge.

Table 3

Cell Parameters for Cathode Limited Cells

Cell No.	Cell Configuration	Carbon Electrode			Lithium Electrode		Electrolyte $LiAlCl_4/SOCl_2$		
		Average Thickness (mm)	Total ARea Facing Li (cm^2)	Approximate Amount of Carbon (mg)	Area (cm^2)	Amount (Ah)	Con. $LiAlCl_4$ (M)	Vol. (ml)	Discharge Current (mA)
P-29	Li/C/Li/C/Li/C/Li (CL*)	0.66	36	400	36	2.01	1.8	4	36
P-35	CL	0.62	36	380	36	2.01	1.8	4	36
P-36	CL	0.62	36	360	36	2.01	1.8	4	36
P-34	CL	0.66	36	420	36	2.01	1.8	4	36**

*CL → cathode limited.
**The cell was charged.

Table 4

Analytical Test Summary of Cathode Limited Cells

Cell No.	Cell Capacity (mA)	Test Performed After: Discharge, mAh IR	Discharge, mAh CV	Overdischarge, mAh IR	Overdischarge, mAh CV
P-29	920	-	-	3240	
P-35	1230	-	-	1872	1872
P-36	1210	-	-	1080	1080
P-34	Cell was charged	-	-	4600	4600

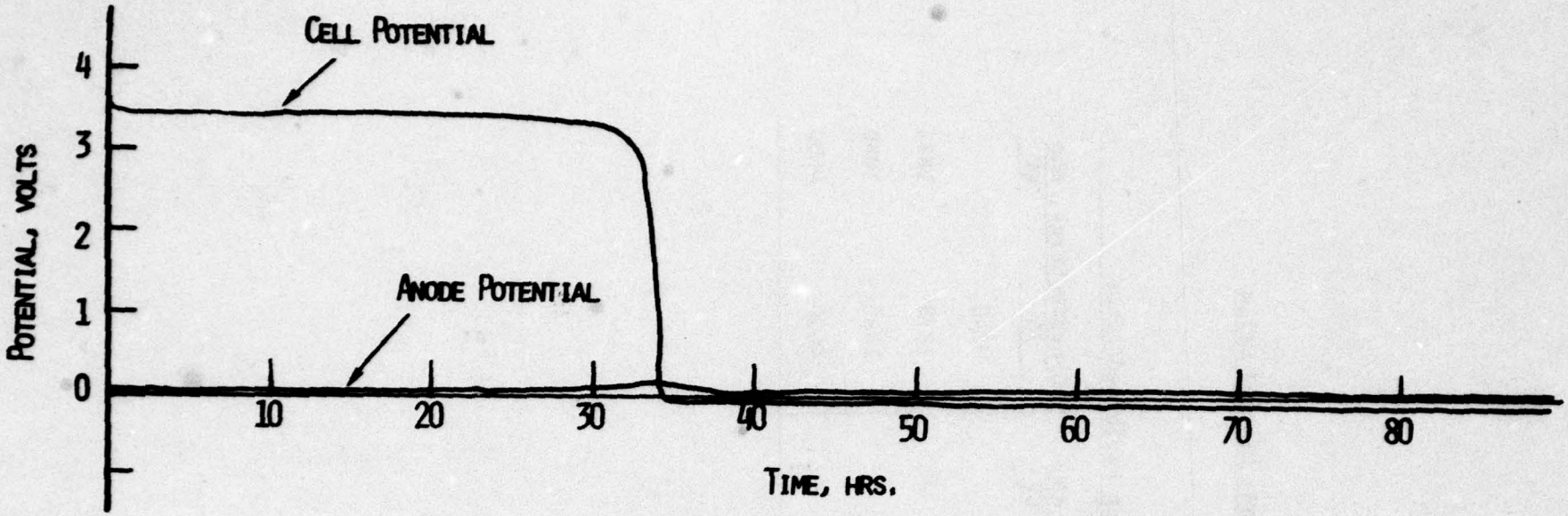

Fig. 25. Discharge and overdischarge curves for cell P-35. Current = 36 mA.

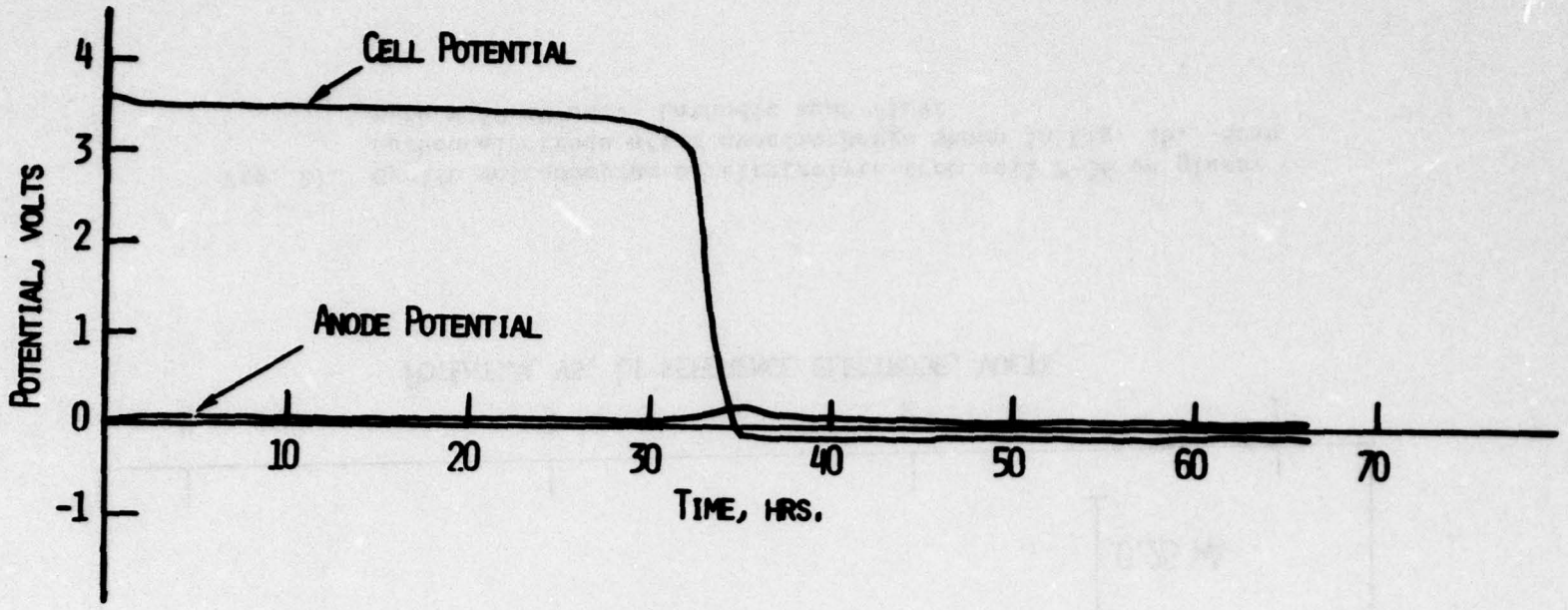

Fig. 26. Discharge and overdischarge curves for Li/$SOCl_2$ cell P-36. Current = 36 mA.

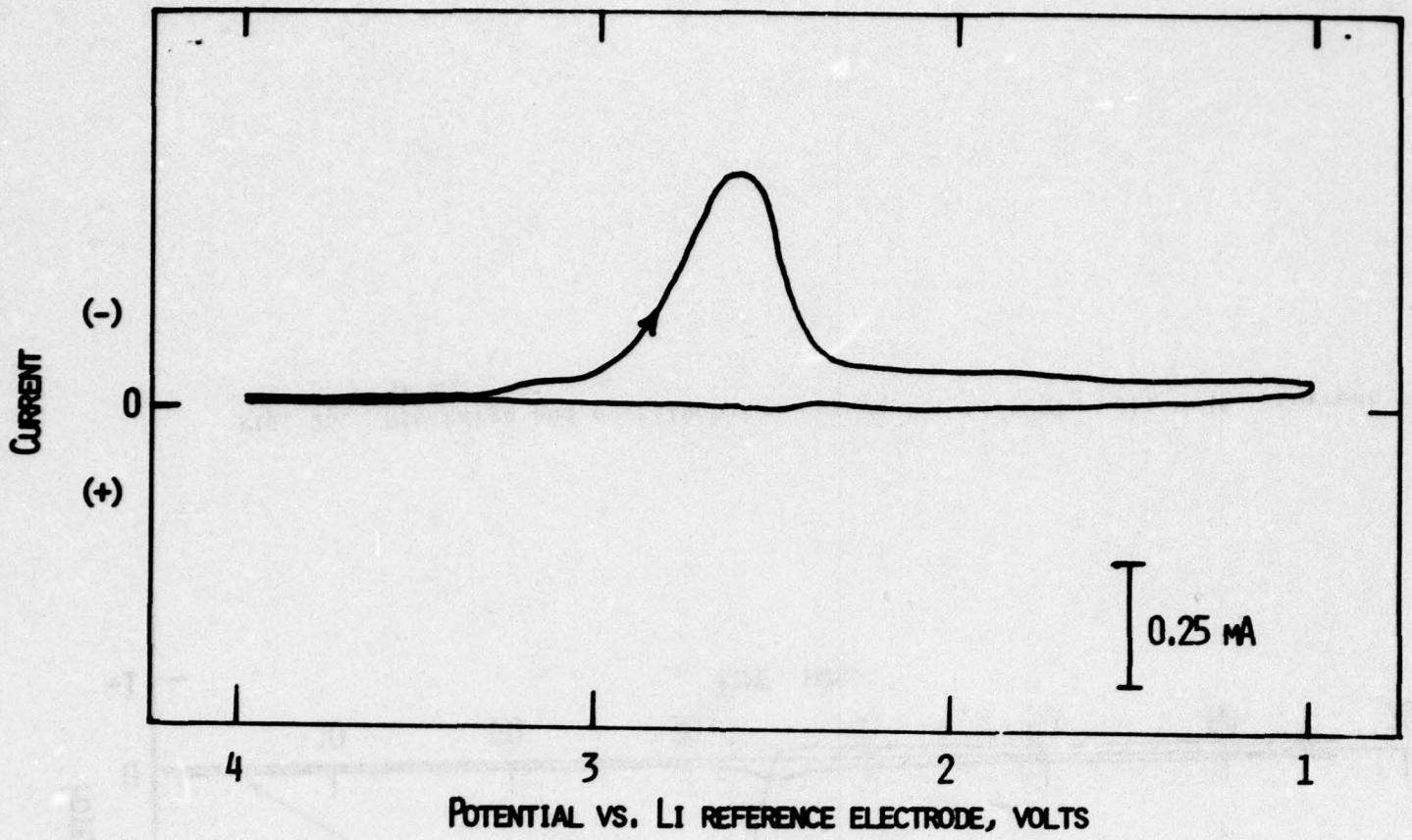

Fig. 27. Cyclic voltammogram of electrolyte from cell P-36 on glassy carbon electrode after overdischarge shown in Fig. 26. Scan rate = 50 mV/sec. Cathodic scan first.

The IR spectrum of the electrolyte from P-36 is shown in Figure 28. The spectrum shows the SO_2 peaks at 1340 cm^{-1} and 1155 cm^{-1}. A weak shoulder is present at 1065 cm^{-1} and two strong bands are present at 790 cm^{-1} and 665 cm^{-1}. The latter bands are quite pronounced and found predominantly in solution from cathode limited cells after overdischarge. All the three cells showed the peaks at 790 cm^{-1} and 665 cm^{-1} in the electrolyte after overdischarge. Partially discharged cells showed these peaks sometimes as weak bands. Isolation experiments showed that the peak is not present in $SOCl_2$/$LiAlCl_4$ solutions, but was found in a solution of Li_2S in $SOCl_2/LiAlCl_4$.

2.3. "Charged" Li/$SOCl_2$ Cells

In order to characterize the reactions responsible for regenerative processes in the "charging" of Li/$SOCl_2$ cells, both cyclic voltammogram and IR spectra were obtained for the electrolyte from cell P-34. The cell had been charged to 4.6 Ah as shown in Figure 29. The cyclic voltammogram is shown in Figure 30. The voltammogram shows the peak due to SCl_2 at 3.65V. A Cl_2 peak may be hidden in the saddle between the two large peaks. IR spectrum, presented in Figure 31, shows SO_2Cl_2 and the product exhibiting the peak at 1070 cm^{-1}. Some SO_2 is also present.

3. Discussion of Analytical Results

Cyclic voltammetry and IR spectral data indicate that SO_2 is produced in Li/$SOCl_2$ cells during the early stages of discharge. Cyclic voltammetry also indicated that LiCl is a product of discharge. These observations are in agreement with the generally accepted discharge mechanisms shown in Equation 1. The often proposed intermediate, SO, could not be identified either by IR spectrometry or cyclic voltammetry.

When anode limited cells are forced overdischarged, the anode potential rises to values >4V leading to oxidation reactions of cell materials with the formation of several products. The oxidation products identified were Cl_2 by cyclic voltammetry and a material absorbing at 1070 cm^{-1} in the infrared spectrum. In some cells small amounts of SO_2Cl_2 and $SOCl^+AlCl_4^-$ were also found. All these products could result from oxidation reactions of the type discussed in the previous section.

Several IR experiments with reagent combinations were performed to identify the material exhibiting absorption at 1070 cm^{-1} in the IR spectrum. Only the spectrum of S_2Cl_2 showed a weak band at 1070 cm^{-1}. This is the first overtone band of the S-Cl stretch at 550 cm^{-1}. However, the intensity of the peak at 1070 cm^{-1} in the electrolyte from cells is much higher than even in neat S_2Cl_2 indicating that the material is different. SCl_2 does not have any absorptions at 1070 cm^{-1}. The possibility of SO_3 was investigated by spectral measurements on solutions of SO_3 in $SOCl_2$. However, SO_3 oxidized $SOCl_2$ rapidly to produce SO_2Cl_2 and no absorption at 1070 cm^{-1} was found. Further studies are in progress to identify this material.

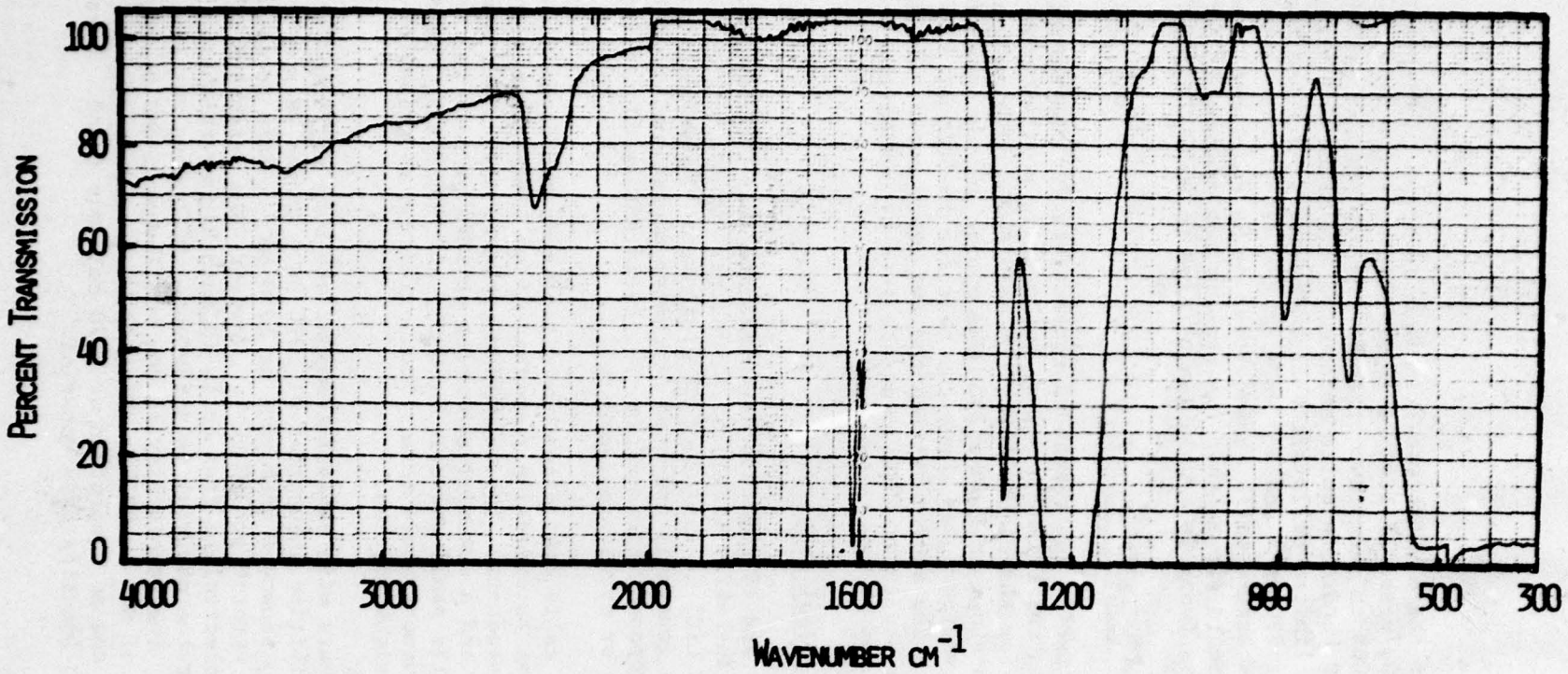

Fig. 28. Infrared spectrum of electrolyte from Li/$SOCl_2$ cell P-36 after forced overdischarge shown in Fig. 26.

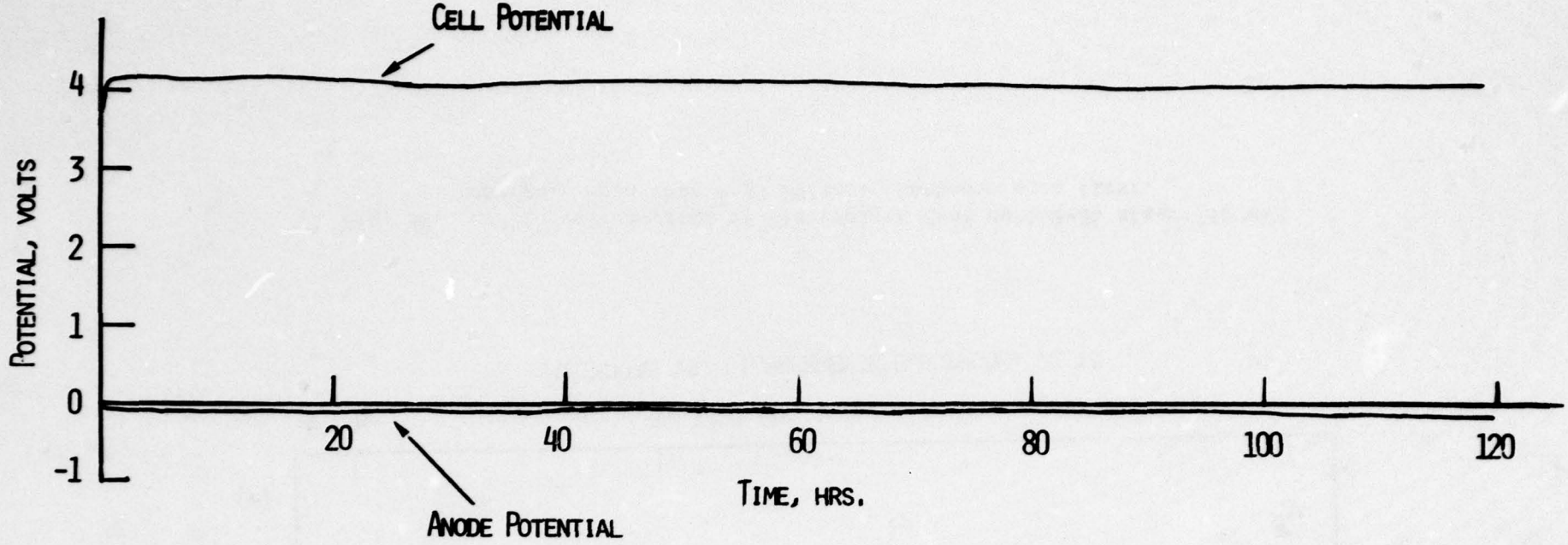

Fig. 29. Galvanostatic "charging" wave for Li/$SOCl_2$ cell P-34. Current = 36 mA.

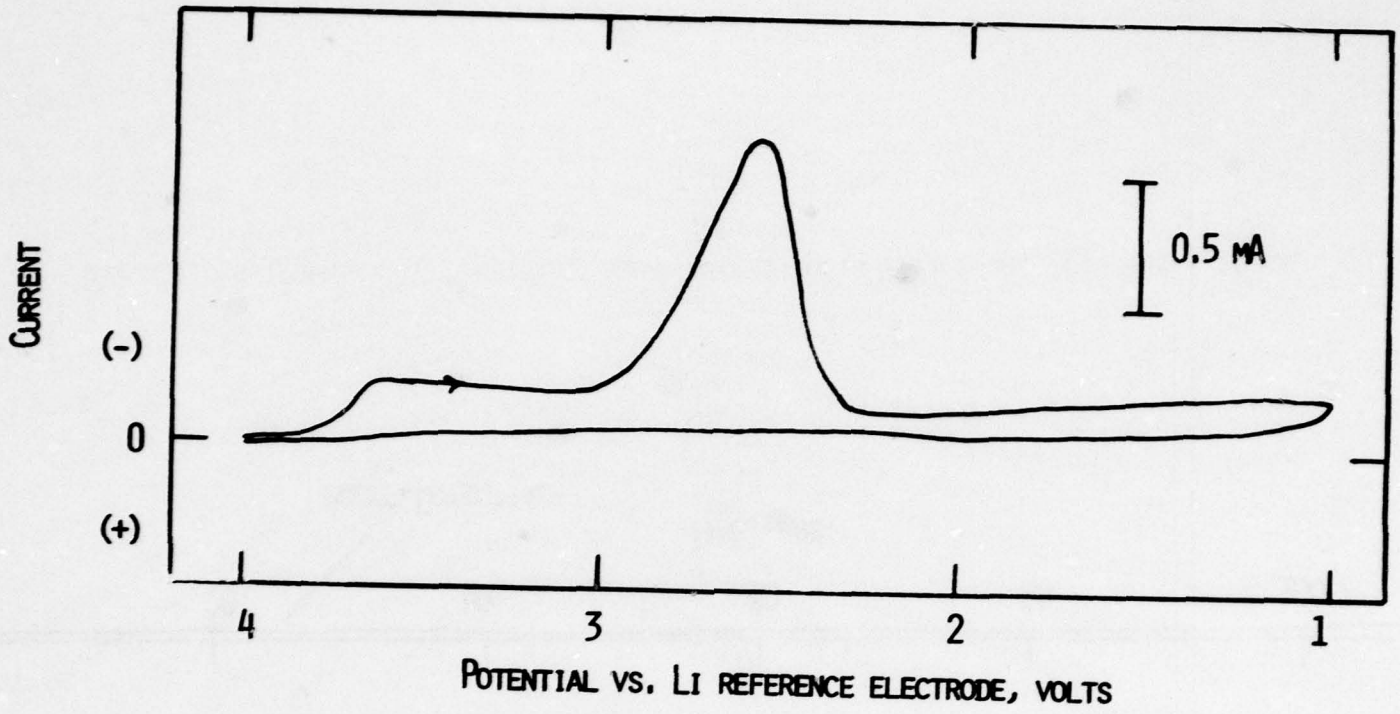

Fig. 30. Cyclic voltammogram of electrolyte from cell P-34 after 750 mAh charge. Scan rate = 50 mV/sec. Cathodic scan first.

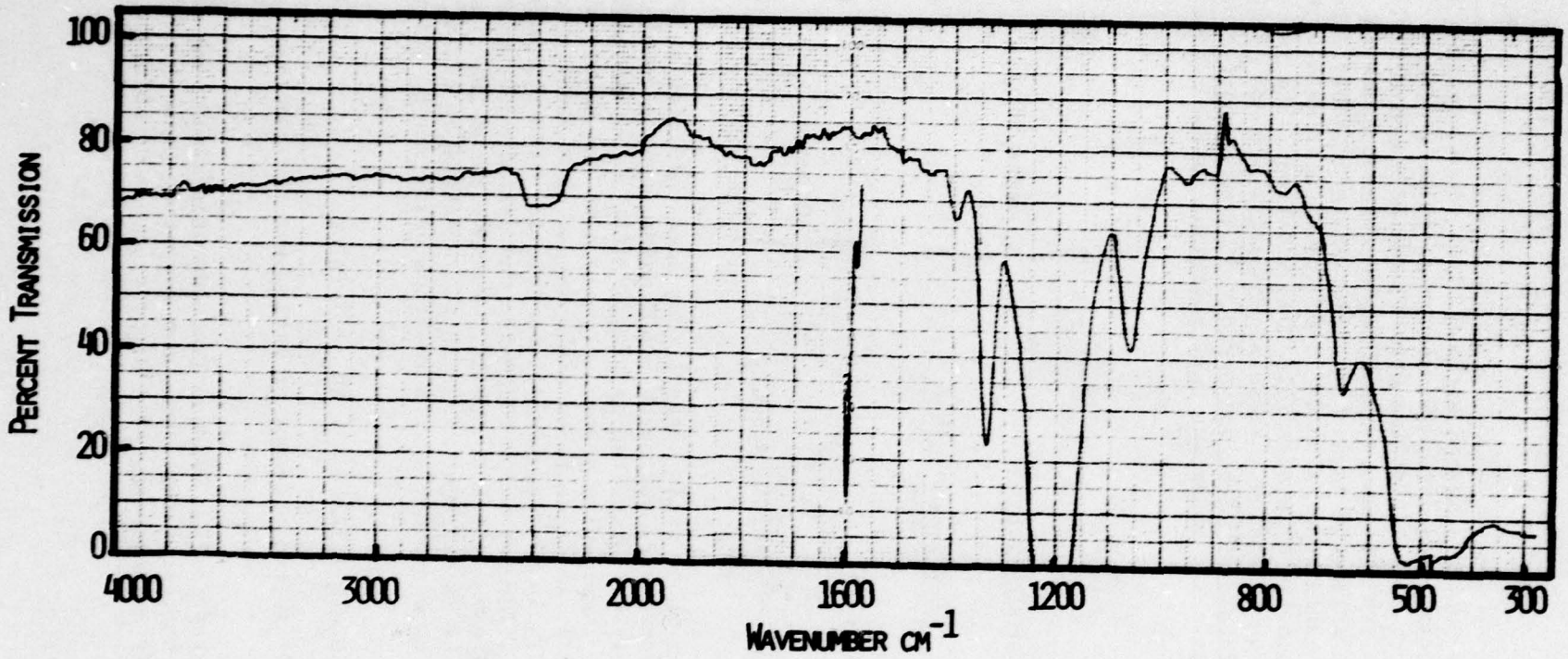

Fig. 31. Infrared spectrum of electrolyte from cell P-34 which was charged shown in in Fig. 29.

In solutions from cell discharged without Li on the anode, SO_2Cl_2, $SOCl^+AlCl_4^-$ and the material exhibiting absorption at 1070 cm^{-1} were identified from IR spectra. Cyclic voltammetry showed SCl_2 and Cl_2 also. The fact these materials are present in much higher concentrations in these cells than in overdischarged anode limited cells is probably due to the absence of Li which could react with the products as well as due to the availability of larger amounts of electrolyte for oxidation. The reaction in the cells without Li on the anode involve regenerative process so that these cells could be "discharged" for long periods of time without changes in electrode polarization. The important cell reactions in the regenerative process may be,

$$AlCl_4^- \rightarrow AlCl_3 + \tfrac{1}{2}Cl_2 + e^- \qquad (11)$$

$$SOCl_2 + AlCl_3 \rightarrow SOCl^+AlCl_4^- \qquad (12)$$

$$SOCl_2 + AlCl_4^- \rightarrow SOCl^+AlCl_4^- + \tfrac{1}{2}Cl_2 + e^- \qquad (13)$$

Anode

$$Li^+ + \tfrac{1}{2}Cl_2 + e^- \rightarrow LiCl \qquad (14)$$

$$LiCl + SOCl^+AlCl_4^- \rightarrow LiAlCl_4 + SOCl_2 \qquad (15)$$

Cathode

The presence of SO_2Cl_2 in these cells suggest that some oxidation of $SOCl^+AlCl_4^-$ also occurs. Control experiments suggested SO_2Cl_2 also forms a complex with $AlCl_3$ which could probably be formulated as $SO_2Cl^+AlCl_4^-$. In the infrared spectrum the peak due to the complex absorb very close to the SO_2Cl_2 absorptions at 1410 cm^{-1} and 1205 cm^{-1}, so that these peaks appear as a doublet in the solution spectrum of $AlCl_3$ in SO_2Cl_2. In dilute solutions the separation of the peaks are not clear. The formation of SO_2Cl_2 and its $AlCl_3$ complex may have relevance to the safety of $Li/SOCl_2$ cells. We have found that the reaction of SO_2Cl_2 with Li is extremely fast in the presence of $AlCl_3$. The IR spectrum identified SO_2 as a product of the reaction which may be written as,

$$2Li + SO_2Cl_2 + 2AlCl_3 \rightarrow SO_2 + 2LiAlCl_4 \qquad (16)$$

$SOCl_2$ also reacts with Li in the presence of $AlCl_3$, but the reaction is much slower.

Analysis of electrolyte from cathode limited cells after long periods of overdischarge showed that some reactions were occurring between cell materials. This is clearly evidenced by the IR spectrum of the solution which

shows an absorption of medium intensity at 790 cm^{-1}. This peak is not found or is very weak in the electrolyte, just at the end of discharge. However, we have found a peak of comparable intensity in solutions of Li_2S in $SOCl_2$/$LiAlCl_4$. This indicates that the peak is due to a Li_2S mediated reaction product of $SOCl_2/LiAlCl_4$. The significance is that Li_2S is formed in the cell during forced overdischarge of a cathode limited cell. It is probable that the Li which is plated on to the cathode during overdischarge reacts with S produced in the discharge to form Li_2S. This Li_2S reacts with the electrolyte to form the product exhibiting the absorption at 790 cm^{-1}. Preliminary evidence suggest that $LiAlCl_4$ is necessary for this reaction of Li_2S. The cyclic voltammograms also showed some Cl_2 in the electrolyte. The Cl_2 may come from the Li_2S reaction or the reaction products. A weak absorption at 1065 cm^{-1} indicates that probably some S_2Cl_2 is present. The absorption may be the expected overtone band of the S-Cl stretch at 550 cm^{-1} as found in neat S_2Cl_2.

The reaction products in solution from the "charged" $Li/SOCl_2$ cells were SO_2Cl_2, SO_2, SCl_2 and the product exhibiting the absorption at 1070 cm^{-1}. Very little or no Cl_2 or $SOCl^+AlCl_4^-$ was found. The cell process is regenerative and may involve reactions of the type shown in Equations 11-15. The difference is that the oxidation reactions occur on the carbon electrode. The explanation for the absence of $SOCl^+AlCl_4^-$ and probably Cl_2 may be related to the regenerative reactions. The chlorine which is produced reacts with Li in the presence of $SOCl^+AlCl_4^-$ to produce $LiAlCl_4$ so that no net concentration of these materials is present in solution.

IV. SUMMARY AND FUTURE WORK

Infrared spectral and cyclic voltammetry data indicated that SO_2Cl_2, Cl_2, $SOCl^+AlCl_4^-$, possibly SCl_2 and a material exhibiting infrared absorption at 1070 cm^{-1} are formed in the oxidation reactions of $SOCl_2/LiAlCl_4$ solutions. The combinations of these materials present in electrolytes from cells vary with the modes of operation and configuration of the cells.

Li_2S formation has been established in cathode limited cells during forced overdischarge. However, no Li_2S is found in the cells at the end of normal discharge or in anode limited cells after forced overdischarge.

On the basis of materials characterized, a mechanism has been proposed for oxidation reactions in $SOCl_2/LiAlCl_4$ solutions.

During the next quarter analytical work will continue with cells discharged on resistive load. We will continue the studies of explosion hazard in $Li/SOCl_2$ cells as a function of $LiAlCl_4$ concentration, current density and cell configuration.

V. REFERENCES

1. W. K. Behl, J. A. Christopulos, M. Ramirez and S. Gilman, J. Electrochem. Soc. 120, 1619 (1973).

2. J. J. Auborn, K. W. French, S. I. Lieberman, V. K. Shah and A. Heller, J. Electrochem. Soc. 120, 1613 (1973).

3. A. N. Dey, P. R. Mallory Company, Second Quarterly Report, ECOM-74-0109-2, November 1974.

4. A. N. Dey and P. Bro, Paper No. 32 presented at the Power Sources Conf., Brighton, 1976.

5. A. N. Dey, P. R. Mallory Company, Interim Report, ECOM-74-0109-13, November 1977 and references therein.

6. N. Marincic and A. Lombardi, GTE Laboratory, Final Report, ECOM-74-0108-F, April 1977.

7. W. K. Behl, Proc. 27th Power Sources Symposium, Atlantic City, June 1976.

8. G. E. Blomgren, V. Z. Leger, M. L. Kronenberg, T. Kalnoki-Kis and R.J. Brodd, 11th International Power Sources Symposium, Brighton, 1978.

9. J. P. Gabano and P. Lenfant, Proceedings of the Symposium on Battery Design and Optimization, The Electrochemical Society, Princeton, NJ, 1978.

10. K. M. Abraham, P. G. Gudrais, G. L. Holleck and S. B. Brummer, 28th Power Sources Symposium, Atlantic City, NJ, 1978.

11. K. M. Abraham, G. L. Holleck and S. B. Brummer, Proceedings of the Symposium on Battery Design and Optimization, the Electrochemical Society, Princeton, NJ, 1978.

12. S. N. Nabi and M. A. Khaleque, J. Chem. Soc. 3626 (1965).

Distribution List

Defense Documentation Center (12)
Attn: DDC-TCA
Cameron Station (Bldg. 5)
Alexandria, VA 22314

Commander
Naval Ocean Systems Center
Attn: Library
San Diego, CA 92152 (1)

CDR, Naval Surface Weapons Ctr. (1)
White Oak Laboratory
Attn: Library Code WX-21
Silver Spring, MD 20910

Commandant, Marine Corps (2)
HQ US Marine Corps
Attn: Code LMC
Washington, DC 20380

Rome Air Development Center (1)
Attn: Documents Library (TILD)
Griffiss AFB, NY 13441

Air Force Geophysics Lab/SULL (1)
Attn: S-29
Hanscom AFB, MA 01731

HQDA (DAMA-ARZ-D/ (1)
Dr. F. D. Verderame)
Washington, DC 20310

CDR, Harry Diamond Laboratories (1)
Attn: Library
2800 Powder Mill Road
Adelphi, MD 20783

Director
US Army Materiel Systems (1)
Analysis Actv.
Attn: DRXSY-MP
Aberdeen Proving Ground, MD 21005

CDR, US Army Research Office (1)
Attn: DRXRO-IP
P.O. Box 12211
Research Triangle Park, NC 27709

CDR, US Army Signals Welfare Lab (1)
Attn: DELSW-OS
Vint Hill Farms Station
Warrenton, VA 22186

Commander (1)
US Army Mobility Equipment
Research & Development Com.
Attn: DRDME-R
Fort Belvoir, VA 22060

Commander
US Army Electronics R & D Command
Fort Monmouth, NJ 07703

DELET-P (1)
DELET-DD (1)
DELET-DT (2)
DELSD-L (Tech Lib) (1)
DELSD-L-S (Stinfo) (2)
DELET-PR (5)

Commander
US Army Communications R & D Command
Fort Monmouth, NJ 07703

USMC-LNO (1)

NASA Scientific & Tech. Info (1)
Facility
Baltimore/Washington International
Airport
P.O. Box 8757, MD 21240

Mr. Donald Mortel (1)
AF Aero Propulsion Lab.
Attn: AFAPL-POE-1
Wright-Patterson AFB, OH 45433

Distribution List
(continued)

Mr. Richard E. Oderwald (1)
Department of the Navy
Hqs., US Marine Corps
Code LMC 4
Washington, DC 20380

Commander (1)
Harry Diamond Laboratories
Attn: DELHD-RDD (Mr. A. Benderly)
2800 Powder Mill Road
Adelphi, MD 20783

Electrochimica (1)
2485 Charleston Road
Mountain View, CA 94040
Attn: Dr. Eisenberg

Dr. Hugh Barger (1)
P.O. Box 2232
Davidson, NC 28036

Energy Storage & Conversion Dept. (1)
TRW Systems
One Space Park
Redondo Beach, CA 90278
Attn: Dr. H.P. Silverman

Sanders Associates, Inc. (1)
24 Simon Street
Mail Stop NSI-2208
Nashua, NH 03060
Attn: J. Marshall

Power Conversion, Inc. (1)
70 MacQuesten Pkwy
Mount Vernon, NY 10550
Attn: Stuart Chodosh

Dr. D. Pouli (1)
Portfolio Manager
Hooker Chemicals & Plastics Corp.
M.P.O. Box 8
Niagara Falls, NY 14302

Dr. Leonard Nanis (1)
G207
S.R.I.
Menlo Park, CA 94025

Dr. J. J. Auborn, Rm 1A-317 (1)
Bell Laboratories
600 Mountain Avenue
Murray Hill, NJ 07974

Stonehart Associates, Inc. (1)
34 Five Fields Road
Madison, CT 06443
Attn: Mr. Thomas Reddy

Mr. J. R. Modem (1)
Energy Conversion Branch Code 3642
Naval Underwater Systems Center
Newport Laboratory
Newport, RI 02840

NASA Lewis Research Center (1)
Mail Stop 6-1
21000 Brookpark Road
Cleveland, OH 44135
Attn: Dr. Stuart Fordyce

Mr. Joe McCartney (1)
Naval Undersea Center
Code 608
San Diego, CA 92132

Atlus Corporation (1)
440 Page Mill Road
Palo Alto, CA 94306
Attn: Douglas Glader

J. Bene (1)
MS 488
NASA Langley Research Center
Hampton, VA 23665

Distribution List
(continued)

Mr. Eddie T. Seo (1)
Research and Development Div.
The Gates Rubber Company
999 S. Broadway
Denver, CO 80217

Mr. Sidney Gross (1)
Mail Stop 8C-62
Boeing Aerospace Company
P.O. Box 3999
Seattle, WA 98124

Honeywell Technology Center (1)
Attn: Dr. H.V. Venkatasetty
10701 Lyndale Avenue South
Bloomington, MN 55420

Transportation Systems Center (1)
Kendall Square
Cambridge MA 02142
Attn: Dr. Norman Rosenberg

GTE Laboratories, Inc. (1)
40 Sylvan Road
Waltham, MA 02154

Foote Mineral Company (1)
Route 100
Exton, PA 19341
Attn: Dr. H. Grady

Honeywell, Inc. (1)
104 Rock Road
Horsham, PA 19044
Attn: C. Richard Walk

Eagle-Picher Industries, Inc. (1)
Electronics Division
Attn: Mr. Robert L. Higgins
P.O. Box 47
Joplin, MI 64801

Yardney Electric Company (1)
82 Mechanic Street
Pawcatuck, CT 02891
Attn: Mr. William E. Ryder

P.R. Mallory & Company, Inc. (1)
Northwest Industrial Park
Burlington, MA 01803
Attn: Dr. Per Bro

Exxon Research & Engg. Company (1)
Corporate Research Laboratory
Linden, NJ 07036
Attn: Dr. R. Hamlen

Argonne National Laboratories (1)
9700 South Cass Avenue
Argonne, IL 60439
Attn: Dr. E. C. Gay

GTE Sylvania, Inc. (1)
77 A Street
Needham Heights, MA 02194
Attn: Mr. Richard Pabst

General Motors Corp. (1)
Research Laboratories
General Motors Technical Center
12 Mile and Mounds Roads
Warren, MI 48090
Attn: Dr. J. L. Hartman

Union Carbide Corporation (1)
Parma Research Center
P.O. Box 6116
Cleveland, OH 44101

P.R. Mallory & Company, Inc. (1)
S. Broadway
Tarrytown, NY 10591
Attn: J. Dalfonso

Distribution List
(continued)

North American Rockwell Corp. (1)
Atomics International Div.
Box 309
Canoga Park, CA 01304
Attn: Dr. L. Heredy

General Electric Research (1)
Development Center
P.O. Box 8
Schenectady, NY 12301
Attn: Dr. Stefan Mitoff

The Electric Storage Battery (1)
Company
Carl F. Norburg Research Center
19 W. College Avenue
Yardley, PA 19067
Attn: Dr. A. Salkind

Gulton Industries, Inc. (1)
Metuchen, NJ 08840
Attn: Mr. S. Charlip